

**FABRICATION AND CHARACTERIZATION OF SUBSTRATE MATERIALS
FOR TRACE ANALYTICAL MEASUREMENTS BY SURFACE ENHANCED
RAMAN SCATTERING (SERS) SPECTROSCOPY TECHNIQUE**

By

Pratima Vabbilisetty

Submitted in Partial Fulfillment of the Requirements

for the Degree of

Masters of Science

in the

Chemistry

Program

**YOUNGSTOWN STATE UNIVERSITY
December 2008**

**FABRICATION AND CHARACTERIZATION OF SUBSTRATE MATERIALS
FOR TRACE ANALYTICAL MEASUREMENTS BY SURFACE ENHANCED
RAMAN SCATTERING (SERS) SPECTROSCOPY TECHNIQUE**

Pratima Vabbilisetty

I hereby release this thesis to the public. I understand that this thesis will be made available from the OhioLINK ETD Center and the Maag Library Circulation Desk for public access. I also authorize the University or other individuals to make copies of this thesis as needed for scholarly research.

Signature:

Pratima Vabbilisetty, Student Date

Approvals:

Dr. Joseph B. Simeonsson, Ph.D., Thesis Advisor Date

Dr. Daryl W. Mincey, Ph. D., Committee Member Date

Dr. Timothy R. Wagner, Ph. D., Committee Member Date

Peter J. Kasvinsky, Dean of School of Graduate Studies & Research Date

Abstract:

The detection of various compounds using Surface enhanced Raman Scattering (SERS) from colloidal suspensions of silver and gold colloids has been attempted. Different substrates have been utilized and SERS spectra for R6G, creatinine, imidazole and benzoic acid have been evaluated as a function of time. SERS investigations have been performed using model compounds to allow comparison between the substrates. Different concentrations of R6G have been used for the evaluation of the analytical capabilities. Silver and gold colloids have been prepared and used for SERS measurements and for the fabrication of substrates having a layer of immobilized metal nanoparticles.

ACKNOWLEDGMENTS

Firstly I would like to express my immense gratitude to my research advisor Dr. Josef B. Simeonsson, whose expertise, understanding and patience added considerably to my graduate experience. I thank him for his constant support and encouragement throughout my research work and thesis. This thesis would not have been completed successfully without his help and effort.

I would like to thank my parents and my elder sister whose constant support, love and inspiration gave me the confidence and strength to accomplish my Masters Program.

I would like to thank my committee members, Dr. Daryl Mincey and Dr. Timothy R. Wagner for their support and assistance throughout my academic career. I would also like to thank the Department of Chemistry and the Graduate School, Youngstown State University for providing funding throughout my Masters program.

Finally, I would like to give special regards to all my friends who encouraged me in all aspects of life. Especially grateful to my best buddy Anand, who was always there with me in every walk of my life.

TABLE OF CONTENTS

TITLE PAGE	i
SIGNATURE PAGE	ii
ABSTRACT	iii
ACKNOWLEDGEMENTS	iv
TABLE OF CONTENTS	v
LIST OF FIGURES	viii
LIST OF TABLES	xii
LIST OF SYMBOLS AND ABBREVIATIONS	xiii
1.0 INTRODUCTION	01
1.1 Raman Spectroscopy	01
1.2 Surface Enhanced Raman Scattering (SERS) Spectroscopy	04
1.2.1 Raman signal Enhancement	07
1.3 UV -Vis Spectrophotometry	08
1.4 Raman Instrumentation	09
1.5 Monochromator	09
1.6 Laser	10
1.7 Fiber Optics	12
1.8 Compounds of Interest	12
1.9 Calibration Curve	14
1.10 Limit of Detection (LOD)	15
2.0 EXPERIMENTAL	16
2.1 Chemicals	16
2.2 Preparation of Colloids	16

2.2.1 Preparation of Gold Colloids	17
2.2.2 Preparation of Silver Colloids	17
2.3 Alternative method for the preparation of Colloids	17
2.3.1 Silver Colloids	17
2.4 Preparation of Substrates	18
2.4.1 Microscopic Glass slides	18
2.4.2 Poly-l-Lysine Slides	18
2.3 Instrumentation	19
2.3.1 Near infra red/Red Laser	20
2.3.2 Visible/Green Laser	20
2.3.3 UV-Vis Spectrophotometer	21
2.4 Safety warnings and precautions	22
2.5 Sample Preparation and procedure	23
3.0 RESULTS AND DISCUSSION	25
3.1 Calibration of Raman Spectra	26
3.2 Rhodamine 6G	28
3.2.1 R6G with Silver Colloid	29
3.2.1.a Calibration curve	31
3.2.1.b Absorbance Spectra enhancement effect	31
3.2.2 Gold colloids with R6G	36
3.3 Creatinine	36
3.3.1 Normal Raman Spectra for Creatinine	37
3.3.2 Creatinine with Silver colloids	38
3.3.2.a Calibration Curve	39

3.3.2.b Absorbance spectra and enhancement effect of Creatinine with silver colloids	40
3.3.3 Creatinine with Gold Colloids	44
3.3.3.a Absorbance spectra and enhancement effects with gold colloid	46
3.4 Imidazole	49
3.4.1 Normal Raman spectra of Imidazole	50
3.4.2 Imidazole with Silver colloid	52
3.4.2.a Calibration curve of Imidazole in silver colloids	53
3.4.2.b Absorbance spectra and enhancement effect	55
3.4.3 Imidazole with Gold colloid	59
3.4.3.a Absorbance spectra and enhancement effect for Imidazole in gold colloid	60
3.5 Benzoic Acid	65
3.6 Microscope Slides	66
3.7 Poly-l-lysine slides	70
4.0 CONCLUSIONS	73
5.0 FUTURE STUDIES	74
6.0 REFERENCES	75

LIST OF FIGURES

Figure (1) Normal scattering of light	02
Figure (2) Raman Scattering Process	02
Figure (3) Monochromator	10
Figure (4) Calibration Curve	15
Figure (5) Setup of SERS Instrumentation	20
Figure (6) UV-Vis Spectrophotometer	22
Figure (7) Raman spectrum of Naphthalene	27
Figure (8) Calibration Curve for frequency standards of Naphthalene	28
Figure (9) SERS spectra for R6G (1 μ M) at 0 min and 5 min after activator addition	30
Figure (10) SERS spectra for R6G at different concentrations at 5 min after activator addition	30
Figure (11) Calibration curve of Rhodamine 6 G in silver colloid	31
Figure (12) Absorbance spectra of R6G at 650 nm	33
Figure (13) Absorbance spectra of R6G at 900 nm	34
Figure (14) Enhancement effect on R6G with silver colloids	35
Figure (15) Normal Raman spectra for Creatinine (20 mM) solution at 65 sec integration time	37
Figure (16) Spectra for Creatinine in different forms	38

Figure (17) Creatinine SERS measurements in silver colloids at 0 min at 10 sec integration time	39
Figure (18) Calibration curve for creatinine in Ag + NaCl at 0 min at 10 sec integration time	40
Figure (19) Absorption Spectra of Creatinine in Silver Collide at 650 nm	41
Figure (20) Absorption Spectra of Creatinine in Silver Collide at 900 nm	43
Figure (21) Enhancement effect of Creatinine in silver colloid	44
Figure (22) SERS spectra for Creatinine in gold colloid at 60 sec integration time at 0 mins	45
Figure (23) SERS spectra for Creatinine in gold colloid at 60 sec integration time at 5 mins	45
Figure (24) Absorbance values for Creatinine in gold colloid at 650 nm	46
Figure (25) Absorbance spectra for Creatinine in gold colloid at 900 nm	48
Figure (26) Enhancement effect of Creatinine in gold colloid	49
Figure (27) Normal Raman spectra for Imidazole	51
Figure (28) Spectra for different forms of Imidazole	52
Figure (29) SERS spectra of Imidazole at 10 sec at 0 min	53
Figure (30) Calibration curve for Imidazole at 1138 cm^{-1} at 10 sec integration time at 0 min	54

Figure (31) Calibration curve for Imidazole at 1234.88 cm^{-1} at 10 sec integration time at 0 min	55
Figure (32) Absorbance spectra for Imidazole in silver colloid at 650 nm	56
Figure (33) Absorbance spectra for Imidazole in silver colloid at 900 nm	57
Figure (34) Enhancement effect for Imidazole in silver colloid at 1138 cm^{-1}	58
Figure (35) Enhancement effect for Imidazole in silver colloid at 1234.88 cm^{-1}	59
Figure (36) SERS spectra for Imidazole in gold colloid at 0 min at 30 sec integration time	60
Figure (37) Absorbance spectra for Imidazole in gold colloid at 650 nm	61
Figure (38) Absorbance spectra for Imidazole in gold colloid at 900 nm	63
Figure (39) Enhancement effect for Imidazole in gold colloid at 1138 cm^{-1}	64
Figure (40) Enhancement effect for Imidazole in gold colloid at 1234.88 cm^{-1}	64
Figure (41) Benzoic acid with 2% NaNO_3 at 120 sec integration time at 0 min	66
Figure (42) Absorbance spectra of gold nanoparticles on glass slides at different wavelengths	67
Figure (43) Absorbance spectra of silver nanoparticles on glass slides at different wavelengths	68

Figure (44) Absorbance spectra of gold nanoparticles on glass slides after acid wash at different wavelengths	69
Figure (45) Absorbance spectra of silver nanoparticles on glass slides after acid wash at different wavelengths	70
Figure (46) Absorbance spectra of silver metal nanoparticles on poly-l-lysine slides	71
Figure (47) SERS measurements of R6G on poly-l-lysine slides with silver nanoparticles at different concentrations	72

LIST OF TABLES

Table (1) Maximum intensities of naphthalene at corresponding pixel numbers.....	27
Table (2) Absorbance values of R6G at 650 nm.....	32
Table (3) Absorbance values of R6G at 900 nm.....	33
Table (4) Enhancement values of R6G with silver colloid at different concentrations.....	35
Table (5) Absorbance values of Creatinine in silver colloid at 650 nm.....	41
Table (6) Absorbance values of Creatinine in silver colloid at 900 nm.....	42
Table (7) Enhancement effect values of Creatinine in silver colloid.....	43
Table (8) Absorbance values of Creatinine in gold colloid at 650 nm.....	46
Table (9): Absorbance values of Creatinine in gold colloid at 900 nm.....	48
Table (10): Absorbance values for Imidazole in silver colloid at 650 nm	56
Table (11): Absorbance values for Imidazole in silver colloid at 900 nm.....	57
Table (12): Absorbance values for Imidazole with gold colloid at 650 nm	61
Table (13): Absorbance values for Imidazole in gold colloid at 900 nm	62

LIST OF SYMBOLS AND ABBREVIATIONS

μL	Micro liters
μM	Micro Molar
μm	Micro meter
$^{\circ}\text{C}$	Degree centigrade
a.u	Atomic units
Ag	Silver
AgNO_3	Silver nitrate
APTES	Aminopropyl triethoxy silane
Au	Gold
CCD	Charge couple device
cm	Centimeter
Cu	Copper
CW laser	Continuous wave laser
HAuCl_4	Tetrachloroaurate
HCl	Hydrochloric acid
HNO_3	Nitric acid
In	Indium
K	Potassium
KHz	Kilo Hertz
Li	Lithium
LOD	Limit of detection
LOQ	Limit of quantification
mL	Milli liter

mM	Milli Molar
mW	Milli Watts
NaCl	Sodium chloride
NaNO ₃	Sodium nitrate
NIR	Near Infrared
PABA	Para amino benzoic acid
PMT	Photomultiplier tube
PNBA	Para nitro benzoic acid
ppb	Parts per billion
ppm	Parts per million
Pt	Platinum
R6G	Rhodamine 6 G
Rh	Rhodium
SERS	Surface Enhanced Raman Scattering
UV-VIS	Ultraviolet-visible
V	Volts

1.0 INTRODUCTION

1.1 Raman Spectroscopy:

The Raman Effect was first reported by the Indian Physicist Sir C.V. Raman in the year 1928. Raman scattering is the inelastic scattering of light by the molecules. In general, when light is scattered by atoms or molecules it obeys the principle of Rayleigh scattering or elastic scattering. In this process the energy and wavelength of the incident photons and the scattered photons is the same. Figure 1 shows the process of Rayleigh scattering.

In the case of Raman scattering, the energy and the wavelengths of the incident and scattered photons are different. This energy difference between the incident light and the Raman scattered light is usually equal to the energy involved in changing the molecule's vibrational state (Figure 2). This energy difference is called the Raman shift. Raman scattering occurs when there is an exchange of energy between the photon and the molecule, leading to the emission of another photon with a different frequency to the incident photon. This inelastically scattered light results due to the changes occurring in the molecular motions. The Raman Effect occurs when the incident light excites the molecules in the analyte due to which scattering of light takes place.

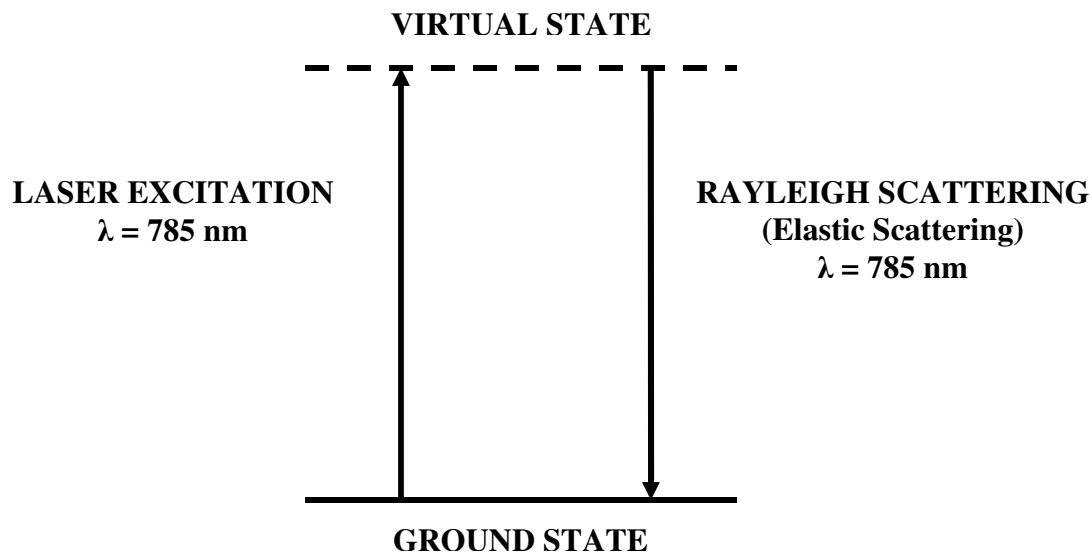


FIGURE 1 NORMAL SCATTERING OF LIGHT

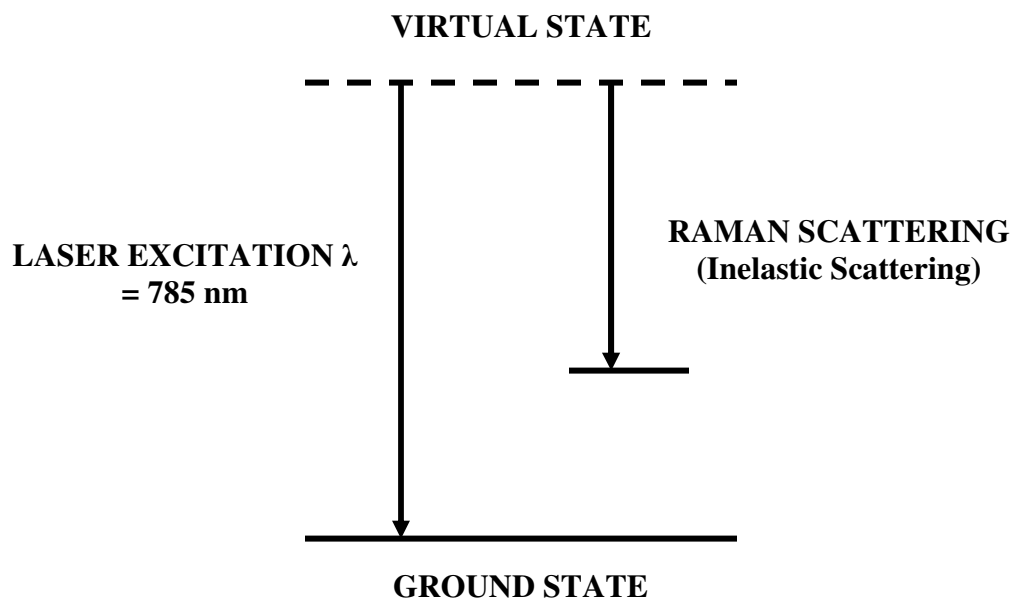


FIGURE 2 RAMAN SCATTERING PROCESS

Raman spectroscopy is the measurement of the wavelength and intensity of inelastically scattered light from molecules. Both Raman spectroscopy and IR spectroscopy measure the vibrational energies of molecules based on different parameters and provide complementary information. Infrared spectroscopy gives information on the changes occurring in the dipole moment of the molecule whereas Raman spectroscopy results from changes occurring in the polarizability of the molecules with the changes in the vibrational motion.

Raman spectroscopy is useful in structure determination, multicomponent qualitative analysis, and quantitative analysis of many compounds. Due to the shift in wavelength of the inelastically scattered radiation, the chemical and structural information of the molecule can be determined. This method provides specific vibrational information for the chemical bonds in molecules and it provides a fingerprint from which the molecule can be identified. It is used to study changes in chemical bonding of molecules and also to determine bond lengths in non-polar molecules. The molecules without a permanent dipole moment can be analyzed by using Raman spectroscopy. Though Raman spectroscopy has many uses and applications in different fields, this process is very weak.¹ This has led to the development of a newer and a better method called Surface enhanced Raman scattering (SERS) spectroscopy in which the scattering is enhanced by 10^3 to 10^7 using² silver and gold nanoparticles. The intensity of the Raman signal from the scattering molecule is greatly enhanced under SERS conditions. As a result, low concentrations of Raman active analyte can be detected by SERS. SERS techniques can detect concentrations as low as pico and femto – molar.

1.2 SURFACE ENHANCED RAMAN SCATTERING (SERS) SPECTROSCOPY:

Surface enhanced Raman scattering spectroscopy (SERS) is a vibrational spectroscopy that is able to identify analyte substances by their vibrational bands and is useful when identification of the analyte is important. SERS is both a selective and a sensitive method. The instrument includes a laser for excitation, a spectrograph and a detector for recording the spectra obtained. It can be a very sensitive spectroscopy that allows the detection of organic molecules adsorbed on noble metal surfaces at sub-micromolar concentration. The two phenomena believed to be responsible for SERS are large increases in the electric field near the surface (electromagnetic effect) and specific adsorbate – surface interactions (chemical effect).^{3,4,5,6} The electromagnetic mechanism takes place only when the localized surface plasmons on the metal get excited. These localized surface plasmons are excited when the incident light strikes the metal surfaces. When the plasmon frequency is in resonance with the radiation, the field enhancement is seen to be the greatest. Scattering of the light takes place when the plasmon oscillations are perpendicular to the metal surface. This effect is strongest where the particle has the highest curvature. As a result, the magnitude of SERS enhancement is highly affected by the adsorption of the analyte on the long or narrow axis of an ellipsoid or spheroid shaped metal particle.

Of the two mechanisms, the chemical effect is believed to contribute only one or two orders of an order or two of magnitude towards surface enhancement. The molecule adsorbed onto the roughened surface of the substrate interacts with the surface of the metal particles. Due to this interaction, metal – adsorbate complexes are formed.^{7,8,9} These complexes produce charge – transfer intermediates that have higher

Raman scattering cross – sections than the analyte that is not adsorbed on the surface. Substrates can include a range of materials and structures. The roughness of the surface is important for large surface enhancements for molecules adsorbed at noble metal surfaces. The degree of enhancement is dependent on the nanometer-scale roughness and optical properties of the substrate employed. Enhancements in Raman scattering between 10^4 and 10^6 are often reported. Enhancements in this range allow SERS to be used in the detection of trace compounds.^{10,11,12,13} Examples of SERS- active surfaces include electrochemically roughened electrodes,¹⁴ microlithographically prepared silver posts, colloidal gold, evaporated thin films, silver coated latex particles, liquid silver films, and substrates prepared by chemical reduction of silver.^{15,16} Among these approaches, metal colloids are commonly used due to their ease of handling and relatively high enhancement factors (usually silver and gold).^{17,18} SERS- substrates made of vapor deposited silver films have exhibited better stability over time, and the substrate performance has been studied as a function of geometry, deposition rate and deposition temperature.^{19,20} The analysis of analytes such as polymers,²¹ dyes,^{22,23} environmental wastes²⁴ and biomolecules²⁵ are some of the applications of SERS.

Surface enhanced Raman scattering (SERS) spectroscopy is a method that can provide valuable vibrational spectroscopy information²⁶ and is capable of very high sensitivity. One of the critical components in an effective SERS measurement is the substrate that provides the surface enhancement. The fabrication of substrates having surfaces that provide strong and reproducible enhancements has been a challenge to the development and application of SERS as a routine analytical method.

The motivation for this research is due to several attractive aspects of SERS as a vibrational spectroscopy, including large signal enhancements compared to solution Raman spectra,^{27,28} high sensitivity, a lack of interference from water, and molecular generality. SERS is a surface sensitive technique. Controlling the size, shape, and structure of metal nanoparticles and their surfaces is important because of the strong correlation between these parameters and optical and electrical properties. As a result, the shape and size of the metal nanoparticles plays a major role in the surface enhancement.

SERS is observed mainly for analytes adsorbed onto (Au, Ag, Cu, Li, Na, or K) metal surfaces, with excitation wavelengths near or in the visible region. Both silver and gold are typical metals for SERS experiments because their plasmon resonance frequencies are in the visible and near infra red regions. Silver and gold nanoparticles can produce enhancements of about 10^8 - 10^{10} for excitation near or in the visible region. The roughness feature of silver and gold nanoparticles is usually on the order of tens of nanometers, which is small compared to the wavelength of the incident excitation radiation. Particles in this size range appear to produce the highest enhancements.

The long term goal of this research is to develop SERS substrates that can be used for sensitive and reproducible measurements at trace levels. The major activities of this research effort have been to evaluate the SERS approach for measurements of several model compounds on silver and gold nanoparticles in solution. In addition, preliminary efforts have been made towards developing SERS substrates based on immobilized metal nanoparticles that can be used for high sensitivity SERS measurements of small samples.

1.2.1 Raman signal Enhancement:

The Raman signal enhancement has been studied by many researchers, of whom Souza *et al*²⁹ have reported the Raman signal enhancement of imidazole on gold colloids. In order to estimate the SERS enhancement, the intensities of the SERS signal are compared with that of the normal Raman intensities. The SERS enhancement effects can be studied or estimated only for compounds that have similar features in both the SERS spectra and the normal Raman spectra. The SERS enhancement effects are calculated by using the following formula. It is the ratio of the Raman intensities normalized by the analyte concentration in samples with and without the presence of colloids (gold / silver).

$$E_{\text{SERS}} = \frac{I_{\text{SERS}}}{C_{\text{SERS}}} \frac{C_{\text{Normal}}}{I_{\text{Normal}}} \quad (1)$$

Where,

E_{SERS} = the Raman signal Enhancement

C_{SERS} = the concentration of analyte solution with gold/silver colloids (Molarity)

C_{Normal} = the concentration of analyte in solution without any gold/silver colloid (Molarity)

I_{SERS} = the SERS intensity (counts)

I_{Normal} = the Raman intensity (counts)

1.3 UV-Vis SPECTROPHOTOMETRY:

UV-Vis Spectrophotometry is used to determine the absorption or transmission of UV-Vis light (180 to 820 nm) by a sample. A UV-Vis spectrophotometer mainly consists of a light source (deuterium arc lamp or an incandescent bulb), a monochromator which produces a monochromatic beam of light, a sample holder or cell, and a detector (usually CCD or a photodiode). For best results, most spectrophotometers use a grating to obtain a specific wavelength of light.

UV-Vis spectrophotometry relies on the principle of light absorption by an analyte, with the amount absorbed (or the percentage of light transmitted) related to the analyte. This is well described by using Beer's law:

$$\log_{10}(P/P_0) = -A \quad \text{or} \quad A = abc \quad (2)$$

Transmittance [(P/P_0)], or absorbance (A), is a function of the constant (a) specific to the substance, the thickness (b), and concentration (c) of the relative number of analyte particles in the light path. Beer's law states that there is a linear relationship between the absorbance (A) and concentration (c) when monochromatic light is used.

The UV – Vis spectrophotometer operates by passing a beam of light through a sample and measuring the intensity of light reaching a detector. The light source is generally a deuterium lamp for UV measurements and a tungsten – halogen lamp for visible and NIR measurements. The detector is generally a photodiode array or a CCD. Monochromators are devices used to obtain light of single wavelength i.e. they produce a monochromatic beam of light. CCDs measure the intensities of light of different wavelengths on different pixels.

The spectrophotometer can be of two types: single beam or double beam. In the case of a single beam instrument, all of the light passes through the cell or sample holder. The Spectronic 20 is an example of a single beam spectrophotometer. In the case of a double – beam spectrophotometer, the light is split into two beams before it reaches the sample. One beam of light is used as the reference and the other beam of light passes through the sample. In some double – beam instruments, two detectors such as photodiodes are used. They detect the signals coming from both the sample and the reference beams at the same time.

1.4 Raman Instrumentation:

The instrumentation in SERS includes a Laser which acts as a light source. The detector consists of a Monochromator and a Charge coupled device (CCD). The Raman instrument may also include fibre optics. The main function of the Raman spectrometer is to reject the intense Rayleigh scattered light and to disperse the Raman scattered light for detection. If the Rayleigh scattered light is allowed to enter the spectrograph unattenuated, it can overwhelm the much weaker Raman scattering spectrum. The most common Raman spectrometers use dispersive gratings and CCD multichannel detectors. These instruments are useful from the UV to the near IR spectral region.

1.5 Monochromator:

The monochromator is an optical device that isolates and transmits a specific band of wavelengths of light. It works on the phenomenon of diffraction of light from a grating. The main components of a monochromator include slits, mirrors and a grating (Figure 3). The monochromator in the Raman spectroscopy instrument uses a CCD as a detector which is located at the exit of the monochromator.

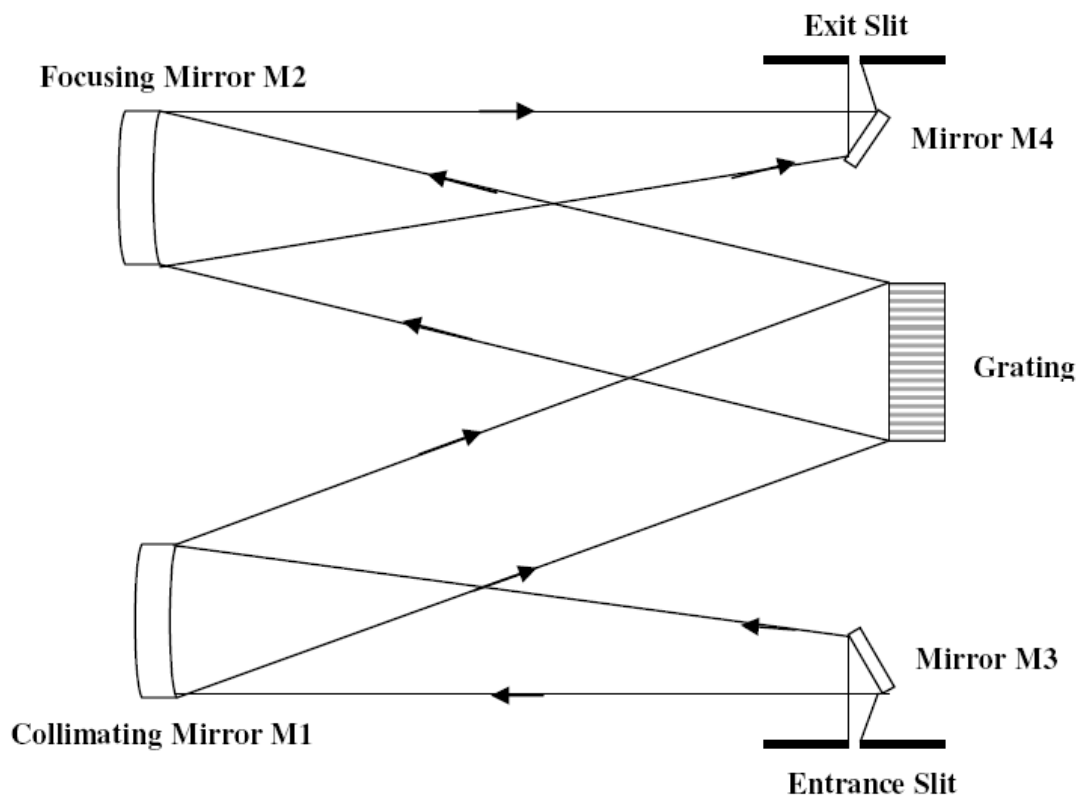


FIGURE 3 MONOCHROMATOR

1.6 LASER:

A LASER acts as the light source in Raman spectroscopy. LASER is an abbreviation for Light Amplification by Stimulated Emission of Radiation. It is an electronic – optical device that produces coherent light radiation. Generally a laser produces light in a narrow, low-divergence monochromatic beam at a specific wavelength. A laser consists of a gain medium that is present in a highly reflective optical cavity which provides energy to the gain medium. The gain medium can be made up of gas, liquid or solid. The cavity consists of two mirrors so that the light bounces back and forth through the gain medium. The output laser beam is emitted through one of the

mirrors which is partially transparent. When the light passes through the laser medium, it gets amplified due to stimulated emission processes.

Laser diodes are semiconductors that convert an electrical current into light emission. This process generates little heat compared to incandescent light sources. These Laser diodes are generally made up of GaAlAs (gallium aluminum arsenide) for short wavelength devices and InGaAsP (indium gallium arsenide phosphide) for longer wavelength devices. In this type of laser, the semiconductor serves as the active medium. The laser diodes are made up from a p-n junction diode that is powered by an injected electrical current. Two types of charge carriers, i.e. holes and electrons, are created when electrical power is applied to the material. The holes from p-doped and electrons from n-doped semiconductors move into the depletion region resulting in light emission. The emitted light is directed towards a reflection mirror and is amplified in the material by stimulated emission. The electrical current determines the amount of amplification and output power in a laser diode. A laser generally operates above the threshold when the gain in energy is high. A semi-conductor crystal can obtain higher gain than a gas laser due to the higher density of atoms available within the gain medium.

The lasers that are used in Raman spectroscopy and SERS techniques are usually visible or near infrared diode lasers. In these studies, the near IR laser emits light of wavelength 785nm. The visible laser emits light of wavelength of 532nm. Both gold and silver colloids give good signals with the near infrared laser but only the silver colloids give good signals with the visible laser light.

1.7 FIBER OPTICS:

Fiber optics are used to direct light from the laser to the sample or from the sample to the detector.³⁰ Fiber optics are made up of glass or plastic fiber and can be used to form optical sensors. The light transmission in the fiber optic probe is based on the principle of Total internal reflection.

1.8 COMPOUNDS OF INTEREST:

Some of the compounds that are reported to give good Raman signals are R6G (Rhodamine species),^{31,32} Benzoic acid,³³ p- aminobenzoic^{33,34} acid and p- nitrobenzoic acid.³⁵ Rhodamine is used as a dye laser gain medium or as a dye in general. It is also used as a tracer dye. Rhodamine produces strong fluorescence and due to this property, it can be easily detected. These dyes are toxic in nature and are soluble in water, methanol and ethanol. Effective SERS cross - sections, however, can be as good as 10^{-18} cm² / molecule for Rhodamine 6G and similar dyes. The Rhodamine dye has high photo stability and a high quantum yield and it is one of the most widely studied probe molecules in SERS techniques.³⁶ Some of the other names for Rhodamine6G are Rhodamine 590, Rh6G, C.I. Pigment Red 169, and Basic Rhodamine Yellow.

Benzoic acid is a colorless crystalline solid. It is an aromatic carboxylic acid. Some of the derivatives of benzoic acid that give good Raman signals are Para amino benzoic acid (4 – Aminobenzoic acid) and paranitro benzoic acid. This is used as a preservative and also as an intermediate in the bacterial synthesis of folate. This compound is mainly used in the manufacturing of esters, folic acid, and azo dyes.

Other compounds that have been measured using the SERS techniques include Creatinine, Imidazole and Benzoic acid (used 532 nm wavelength produced by Visible laser) both in silver and gold colloids using the Infra – red laser at 785 nm wavelength.

Souza *et al*²⁹ have reported the in vitro and in vivo detection of self – assembled Au – Imidazole using near – infra red surface enhanced Raman spectroscopy (NIR – SERS). Due to the presence of two nitrogens in positions they form a bridge between the metal particles³⁷ (gold or silver colloids). Imidazole and its derivatives help in preventing corrosion and they act as precursors for the adsorption of other substances onto metal surfaces. The imidazole ring system is present in important biological molecules such as histidine, nucleic acids, and histamine.

Creatinine is a breakdown product from Creatinine phosphate in the muscle. The concentration or the amount of Creatinine is increased in the urine, due to certain diseases like muscle dystrophy and hyperthyroidism. In order to detect and monitor the presence of such nitrogen containing compounds present in urine, a sensitive technique like SERS has been evaluated for low level detection. By monitoring the amount of Creatinine present in the urine³⁸, the renal function can be monitored and it can act as an internal reference value in urine. Previous studies have shown it is possible to measure 0.5 mg/dL of Creatinine present³⁹ in the urine using SERS techniques. In that work, Sodium borohydride was used for the preparation of colloidal gold solution. An integration time of 10 sec was used for obtaining the spectra and the fiber optic probe was focused directly into the sample solution being measured (urine sample).

1.9 CALIBRATION CURVE:

A calibration curve is a general method for determining the concentration of a substance present in an unknown sample by comparing the unknown to a set of standard samples of known concentrations. This plot provides information about how the analyte signal changes with the changing concentration of the substance to be measured. The graph is plotted by taking the concentrations on the X- axis and the signal on the Y – axis. From this calibration curve it is possible to determine many parameters such as the Limit of detection (LOD), the slope, the intercept, the limit of quantification, the limit of linearity (LOL) and the dynamic range. From linear regression analysis, it is possible to determine the best – fit straight line. The following equation is used:

$$y = mx + c \quad (3)$$

It is then possible to solve for the concentration (x) in an unknown sample by substituting the signal values (y), slope (m), and intercept (c). Uncertainty values can also be calculated from the data obtained in the experiment. The uncertainty from the calibration curves is related to the uncertainty in the regression line. This uncertainty is generally given by the below equation:

$$S_{y/x} = \sqrt{(\sum (d_i)^2 / (N - 2))} \quad (4)$$

Where $S_{y/x}$ = std. deviation of the residuals and is proportional to the uncertainty in the slope (S_m) and the uncertainty in the y – intercept (S_b).

1.10 Limit of Detection:

The Limit of detection is expressed as the concentration or the quantity that is derived from the smallest measure that can be detected for a given analytical procedure.

The units for LOD are usually in units of concentration. The limit of detection can be determined by this equation.

$$\text{LOD} = \frac{3 * \sigma}{m} \quad (5)$$

Where σ = standard deviation of the blank measurements

m = slope of calibration curve.

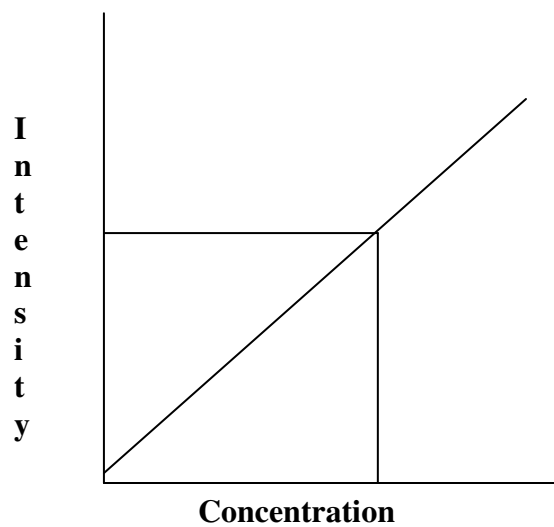


FIGURE 4 CALIBRATION CURVE

2.0 EXPERIMENTAL SECTION:

2.1 CHEMICALS:

Raman studies were performed using several different compounds. Rhodamine species such as Rhodamine 6G were obtained from Lambda Physik. Benzoic acid species such as para aminobenzoic acid and para nitro benzoic acid were obtained from Aldrich. All benzoic acid species samples were stored in the dark. Phenols such as 2-chlorophenol and 4-chlorophenol were also studied in these experiments. Creatinine was ordered from Acros (Organics) and Imidazole was acquired from Aldrich. Suspensions of silver colloids were prepared by using Silver nitrate solutions of concentrations (0.1 N, 1 N conc.). Both Sodium tetrachlorate and silver nitrate were obtained from Aldrich. Aminopropyltriethoxysilane (APTES- 99%) used in the preparation of nanoparticle based substrates was acquired from Aldrich. Aggregating agents such as sodium nitrate, sodium chloride (Certified ACS) and sodium formate were obtained from Aldrich. Trisodium citrate was used for producing metal colloids. The citrate acts as a reducing agent for both the gold and silver of colloids. Glass slides (25mm x 75mm x 1mm) used for the preparation of the glass substrates were acquired from Fisher Scientific. Distilled water was used for all dilutions and preparation of samples. Poly – l- lysine slides were obtained from Sigma Aldrich.

2.2 PREPARATION OF COLLOIDS:

2.2.1 PREPARATION OF GOLD COLLOIDS:

The gold colloids were prepared using a procedure described by Grabar *et al.*⁴⁰ The glassware was washed with aqua regia (3 HCl: 1 HNO₃) and rinsed with distilled water. Sodium tetrachloroaurate (50 mg, BDH) was dissolved in distilled water (500 ml)

and brought to boiling. Then trisodium citrate was added (7.5 ml of 1% sol.) to the boiling solution. After addition of the citrate solution, the color changes from light yellow to dark red, indicating the formation of the gold colloid. It is allowed to boil for 15 mins and then cooled and stored for future use. The obtained gold colloids are estimated to be about 20 nm- 60 nm in size.

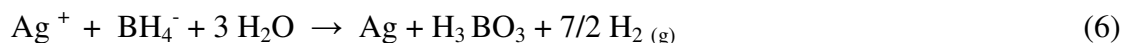
2.2.2 PREPARATION OF SILVER COLLOIDS:

The silver colloids were prepared using a procedure reported by Lee and Meisel *et al.*⁴¹ The glassware was washed with aqua regia (3 HCl: 1 HNO₃) and rinsed with distilled water. A volume of 500 ml of distilled water was placed in a round bottomed flask and heated to 45⁰ C. A mass of 90 mg of silver nitrate was added and stirred. The solution was brought to boiling and then sodium citrate dihydrate (10 ml of 1% sol.) was added. Once the color changed from transparent to grey color, the solution was simmered gently for 90 mins and allowed to cool.

2.3 ALTERNATE METHOD FOR THE PREPARATION OF COLLOIDS:

2.3.1 SILVER COLLOIDS:

The silver colloids were also obtained from the chemical reduction of silver nitrate by sodium borohydride as described by *J. D. Guingab et al.*⁴² Aqueous solution of (2 x 10⁻³ M) sodium borohydride and (1 x 10⁻³ M) silver nitrate solution were mixed at 6:1 (v/v) volume ratio to obtain the silver colloids. The equations 6 and 7 represent the reactions taking place between the above used reagents:



2.4 PREPARATION OF SUBSTRATES:

2.4.1 MICROSCOPE GLASS SLIDES:

Glass slides were washed with aqua regia (3 HCl: 1 HNO₃) and thoroughly washed with ethanol (anhydrous) for about 3 times. Then the glass slides were placed in 10% Aminopropyltriethoxysilane (APTES) solution for 15 mins for the immobilization of the metal particles onto the glass slides. Due to this an amine terminated surface was created for the better binding of the metal nanoparticles onto the glass surface.⁴³ After 15 min, the glass slides were washed again with anhydrous ethanol for 5 times to remove excess of the solution. Then the glass slides were placed in an oven at 120⁰ C for 3 hr for drying. After 3 hr of drying, the dried glass slides were placed in colloidal solutions of gold or silver suspensions and left for about 12 hrs overnight. Once the metal nanoparticles bound onto the surface, they were washed with anhydrous ethanol again and stored in plastic containers either in water or ethanol solutions for future use.

2.4.2 POLY -L- LYSINE SLIDES:

Poly – l- lysine slides were also employed as glass substrates for carrying out the SERs measurements. The use of these pre treated lysine slides avoids procedures like substrate modification. The poly – l- lysine acts as a linker molecule between the glass substrates and the colloids being used. This linkage is due to the formation of strong bonds between amino groups of the l – lysine slides and the colloids. Due to the use of the poly – l- lysine slides, some surface inhomogeneities may be avoided. In the case with the laboratory derivatized microscope slides, there is more chance of variations to occur because the substrate modification is completely operator dependent. However in the case of the poly- l-lysine slides, there is no need to wash and dry the slides as they only need

to be placed in the respective colloids. Poly- l- lysine slides have recently been demonstrated for the detection of Rhodamine 6G and Isoniazid compounds in Gold colloids.³⁶

2.5 INSTRUMENTATION:

The Raman instrument consists of a laser which acts as a light source. The detector consists of a monochromator and a Charge coupled device (CCD). The monochromator was used in order to get light of desired wavelength and a CCD is used for detecting the Raman signals. The CCD consists of several small units for detection arranged in rows. The signals were obtained and displayed on the computer (Figure5). Glass slides were used to bind the metal nanoparticles for the preparation of the substrates. Suspensions of silver and gold colloids were prepared for the making of the SERS substrates. The red laser emits light of wavelength of 785 nm and the green laser emits light of wavelength of 532 nm. Absorbance values of the glass substrates obtained were measured by means of a UV-Vis spectrophotometer.

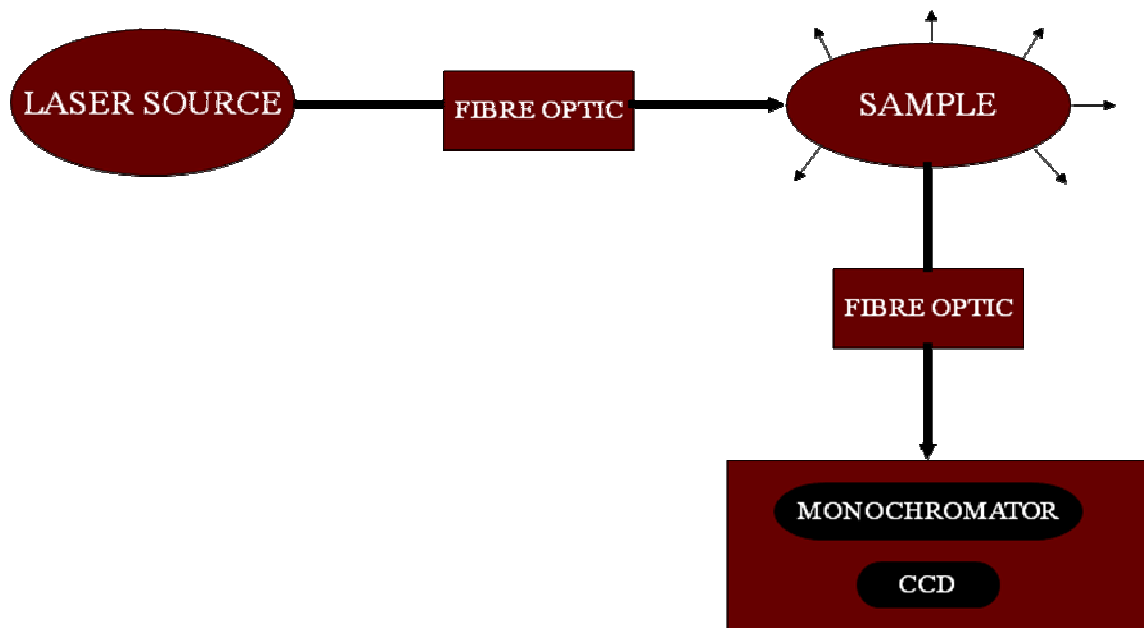


FIGURE 5 SETUP OF SERS INSTRUMENTATION

2.5.1 NEAR INFRA RED / RED LASER:

This detector is a BTC111E Fiber coupled TE cooled linear CCD array Spectrometer. This CCD spectrometer is equipped with a 2048 element detector. The detector has 2048 elements @14 μm x 200 μm and minimum and maximum integration times of 9 ms and 65,535 ms. The red laser operates at an output power between 0-480 mW and a LD operating current of 0.70 A. A fiber optic probe was used to direct light coming from the laser onto the sample and from the sample to the detector.

2.5.2 VISIBLE/GREEN LASER:

The green laser system is an R-2001(Raman Systems, Inc.) system which includes five basic elements: a diode laser, a fiber – optic probe, a spectrometer, an A/D card, and operating software. The diode laser supplies light through the excitation fiber in the fiber-optic probe. The scattered light from the sample is collected and transmitted to the

spectrometer via the collection fibers in the fiber-optic probe. The spectrometer consists of the monochromator and the CCD. The CCD has 2048 elements @ 125 μm x 200 μm per element. The spectrometer measures the amount of light at each pixel in the sampled spectrum. The A/D card transforms the analog data from the spectrometer into digital information that is passed to a computer. Finally, the operating software converts the digital data from the spectrometer into the Raman spectrum. The green laser functions between a minimum and maximum integration time of 1 sec – 4 mins. The grating used in the green laser consists of 1200 lines/mm.

2.6 UV-VIS SPECTROPHOTOMETER:

The UV Vis spectrophotometer uses light in the visible (Vis), near ultraviolet (UV) and near infrared (NIR) ranges to determine the absorbance or transmittance of UV/Vis light by the sample. A beam of light from a visible and/or UV light source is separated into its respective wavelengths by means of a prism or diffraction grating. This instrument measures the intensity of light passing through a sample, and compares it to the intensity of light before it passes through the sample. In these studies, the absorbance or transmittance of light is a measure of the plasmon absorption of the metal nanoparticles. The UV-Vis spectrophotometer used was a Hewlett Packard system.

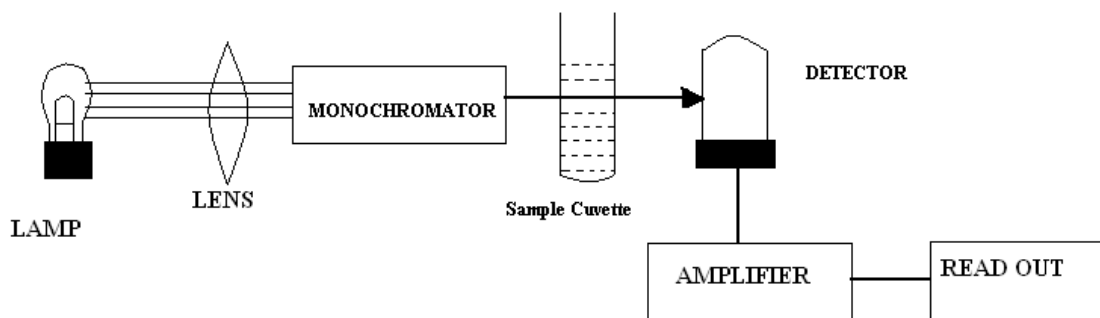


FIGURE 6 UV-VIS SPECTROPHOTOMETER

The absorbance values of the glass substrates were measured by a UV-Vis spectrophotometer. The basic parts of the UV Vis spectrophotometer are a light source (incandescent bulb/ Tungsten lamp or deuterium arc lamp), a holder/cell for the sample, a monochromator (to obtain light of desired wavelength) and a detector (either a photodiode or charge couple device (CCD)) as shown in Figure.6. The spectrophotometer used was a single beam device.

2.7 SAFETY WARNINGS AND PRECAUTIONS:

Phenols and other volatile samples should be prepared and diluted under the hood and gloves are to be worn always while performing the experiments and during handling of the apparatus. The suspensions of colloids are also to be prepared under the hood.

Some safety precautions recommended while operating the laser:

1. Post warnings in the area where the instrument is to be used.
2. Allow access only to authorized personnel.
3. Do not look directly in the path of the beam.

4. Always wear safety goggles while using the system. Goggles which are tuned to 532nm or 785nm are to be worn while operating the laser.

Dark materials and materials that are opaque in the infrared will absorb the laser energy more efficiently than transparent materials. These materials can heat up more quickly and may become more sensitive to ignition and detonation. High laser power focused on a small spot can produce very high power density and cause the sample to burn.

2.8 SAMPLE PREPARATION AND PROCEDURE:

Different concentrations of R6G and benzoic acid (1 mM, 0.5 mM, 0.25 mM, 0.1 mM, 0.01 mM, 0.05 mM, 0.001 mM, 0.003 mM, 0.005 mM, 0.0001 mM) were prepared. They were diluted to different concentrations with methanol solutions. Para nitro benzoic acid and Para amino benzoic acid were also diluted to different concentrations with methanol (100 mM, 50 mM, 10 mM, 1 mM, 0.5 mM, 0.1 mM, 0.01 mM, 0.05 mM). 10%, 1%, 5% solutions of the activators or aggregating agents (such as sodium chloride,⁴⁴ sodium formate, sodium nitrate) were prepared with distilled water. Initially different concentrations of Rhodamine (laser dye) and benzoic acid species were prepared and the SERS measurements were taken in solution form. These measurements were taken at different integration times (1000 ms, 10000 ms, 30,000 ms, 60,000 ms) by the red laser light for a period of one hour with intervals of 5 min. SERS measurements for benzoic acid species were even taken by a green laser light at different integration times (1 s, 10 s, 30 s, 60 s, 120 s).

Substrates were prepared using suspensions of gold or silver metal nanoparticles. The substrates were prepared in combinations of gold and activator, only gold colloid,

silver colloid and activator, and silver colloid only. Some substrates were prepared even by using cover slips instead of glass slides using the same procedure as that of glass substrate preparation mentioned above.⁴⁵ Using the glass substrates, SERS measurements were taken for the R6G dye present on the substrates as a function of the laser power. Some substrates were prepared in a different way by not keeping the glass slides in the respective colloids for 12 hrs. Instead, the glass slides were kept for 8 hrs in the colloids, but, the colloidal solution was replaced with fresh colloid solution for every 2 hrs. Absorbance spectra were obtained for the cover slips substrates and acid washed glass substrates.

3.0 RESULTS AND DISCUSSION

The results of SERS measurements obtained for Rhodamine (R6G), Creatinine, Imidazole, Benzoic acid and Para amino Benzoic acid (PABA) are reported in this section. SERS spectra were obtained for all the compounds in the presence of both silver and gold colloids at different time intervals and different measurement integration times.

SERS spectra were taken for R6G at different concentrations with respect to time following activation of the colloids. Spectra were also taken at different measurement integration times (10 sec, 30 sec, and 60 sec). Calibration curves were obtained using different concentrations of R6G (100 μM , 10 μM , 1 μM , 0.9 μM , 0.7 μM , 0.5 μM , 0.3 μM , 0.1 μM). Limit of detection values were calculated for R6G in the presence of silver colloids from the calibration curves. The linear responses of different concentrations of R6G were determined using the calibration curves. The absorbance and enhancement spectra were studied for R6G in the presence of both gold and silver colloids at different concentrations and time intervals (0 mins-5 mins).

Spectra were also obtained for Creatinine, Imidazole and PABA compounds. Calibrations curves were obtained and the limits of detection values were calculated. The values were compared for the above compounds in the presence of silver and gold colloids.

Glass substrates (gold and silver) were prepared to evaluate their use for SERS and enhancement in the peaks of the Raman intensities. Both gold and silver substrates were prepared and their absorbance spectra were obtained at different wavelengths. Glass substrates based on poly-L-lysine slides were studied for detection of the above

compounds at low concentrations. Absorbance spectra for the silver coated lysine slides and gold coated lysine slides were also obtained.

3.1 CALIBRATION OF RAMAN SPECTRA:

The SERS spectra obtained for all the different compounds were acquired in the form of counts as a function of pixel numbers. Each pixel number represents each unit of the 2048 element CCD detector. These pixel numbers were converted into wave numbers by using the Raman shift frequency standard of naphthalene. A plot was made by using the pixel numbers on the X- axis and the frequency standards on the Y- axis. From this plot, the slope and the Y- intercept of the regression were obtained. The pixel numbers were then substituted in the equation and the resultant Raman shift values were calculated. These values were used in the Raman spectral plots. Figure7 below shows the normal Raman spectrum of Naphthalene (solid form). Table 1 shows the frequency standards of Naphthalene and the observed pixel numbers at maximum intensities. Figure (8) shows the linear plot of the frequency standards of naphthalene as a function of the pixel number.

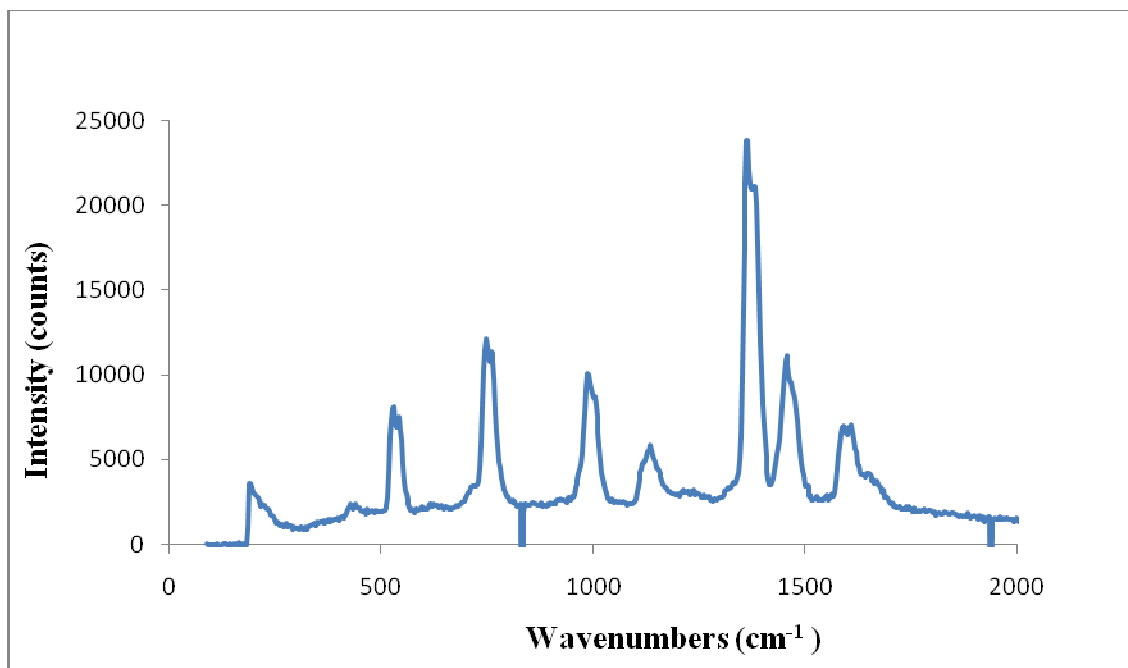


FIGURE 7 RAMAN SPECTRUM OF NAPHTHALENE

Pixel number	Frequency
157	513.8
234	763.8
318	1021.6
450	1382.2
483	1464.5
529	1576.6

TABLE 1: MAXIMUM INTENSITIES OF NAPHTHALENE AT CORRESPONDING PIXEL NUMBERS

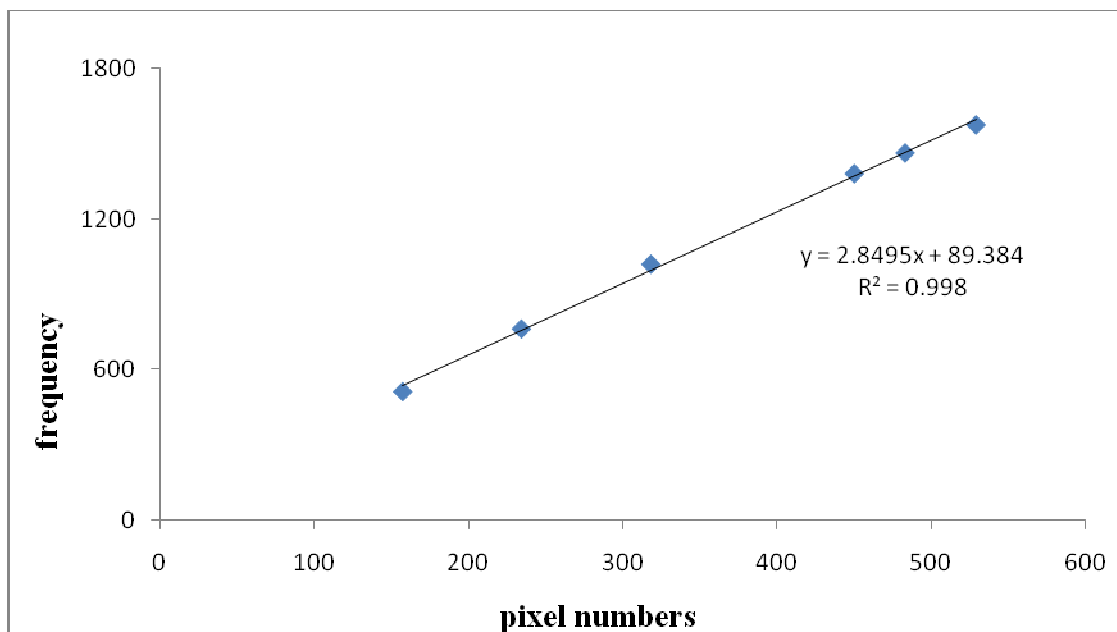


FIGURE 8 CALIBRATION CURVE FOR FREQUENCY STANDARDS OF NAPHTHALENE

3.2 RHODAMINE6G:

The SERS spectra for R6G were obtained by measuring different concentrations at different intervals of time after activation and different integration times. Several measurements were taken for each concentration in order to check the reproducibility of the spectra. Spectra were taken at different integration times to find the highest signal for each concentration. The stock solutions of Rhodamine were prepared by dissolving the compound in ACS grade methanol and all the other lower concentrations were diluted using the same methanol. High intensity values were obtained at 10 sec integration times and at 5 mins after activator addition for silver (Figure 9) and at 0 mins for gold colloids. The intensity varied with the change in the integration time and activator concentration. A 10% NaCl solution was used as the activator and the measurements were obtained at 5 mins. These parameters were kept constant in order to obtain reproducible peaks. Sample

measurement conditions were: 2700 μL of either silver / gold colloid + 300 μL of sample to be detected + 150 μL of activator. The graphs were plotted by taking the wavenumbers on the X- axis and the intensity values on the Y- axis. The maximum intensities for Rhodamine 6G were obtained at two wavenumbers (1346 cm^{-1} and 1519 cm^{-1}).

3.2.1 R6G WITH SILVER COLLOID:

SERS spectra were obtained by taking measurements of the sample (2700 μL of silver colloid + 300 μL of compound + 150 μL activator (10% NaCl)) at different concentrations ranging from 1000 μM – 0.1 μM) at different intervals of time after activation (0 mins, 5 mins) and at different integration times (10 sec, 30 sec, 60 sec). This was done in order to find the maximum intensity and the best linear responses of the concentrations. Figure 10 indicates that there is an increase in the intensity with time after activation for R6G concentrations due to increased aggregation of the colloid. The SERS spectra of R6G at different concentrations at 5 mins as shown in Figure 10 illustrates that linearity could be achieved at lower concentrations ranging from 1 μM to 0.1 μM .

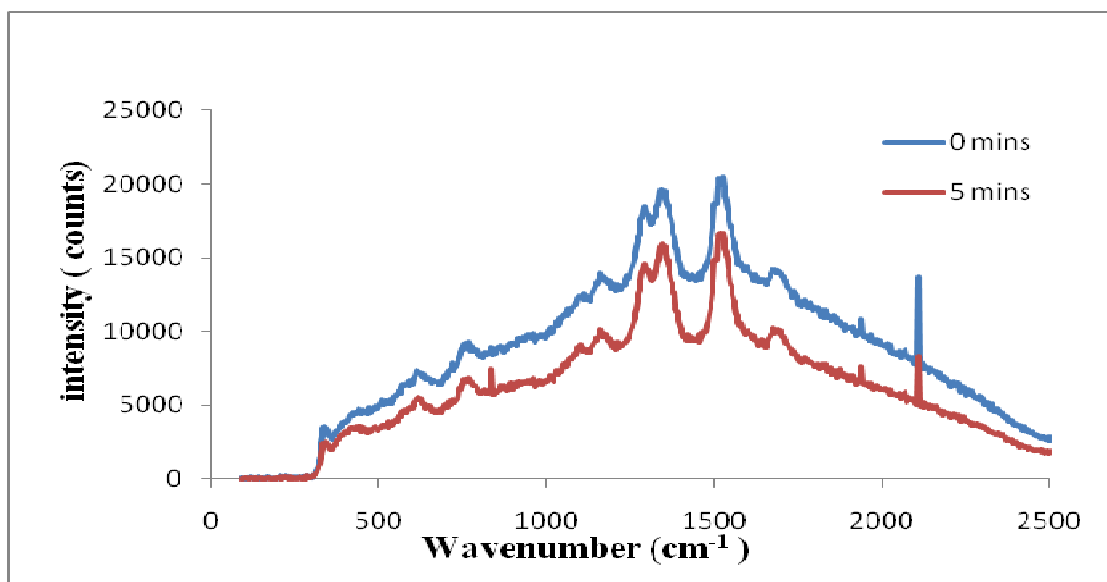


FIGURE 9 SERS SPECTRA FOR R6G (1 μM) AT 0 MINS AND 5 MINS AFTER ACTIVATOR ADDITION

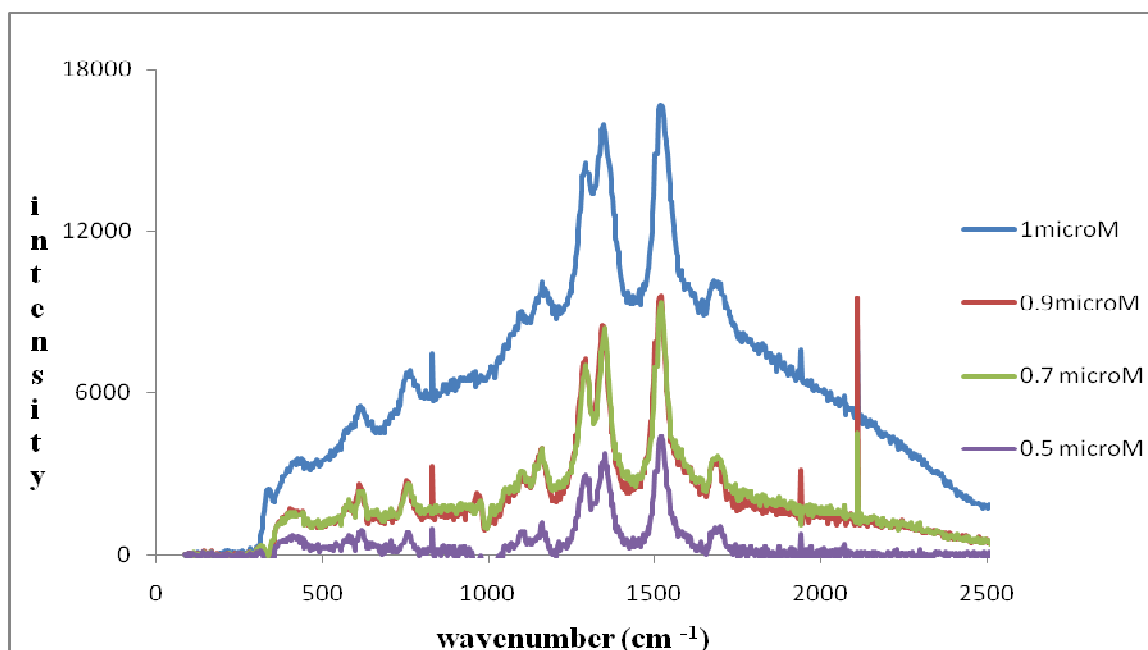


FIGURE 10 SERS SPECTRA FOR R6G AT DIFFERENT CONCENTRATIONS AT 5 MINS AFTER ACTIVATOR ADDITION

3.2.2 CALIBRATION CURVE:

Based on the above spectra, a calibration curve (Figure 11) was plotted for the concentrations ranging from 1 μM to 0.1 μM . The concentrations were taken on the X – axis and the intensities (counts) were taken on the Y – axis. The peak heights were calculated from the intensities obtained at wave number 1346 cm^{-1} . At 5 mins after activator addition, a slope (m) of 6437.9 and a y- intercept value of 707.05 were obtained from the calibration curve.

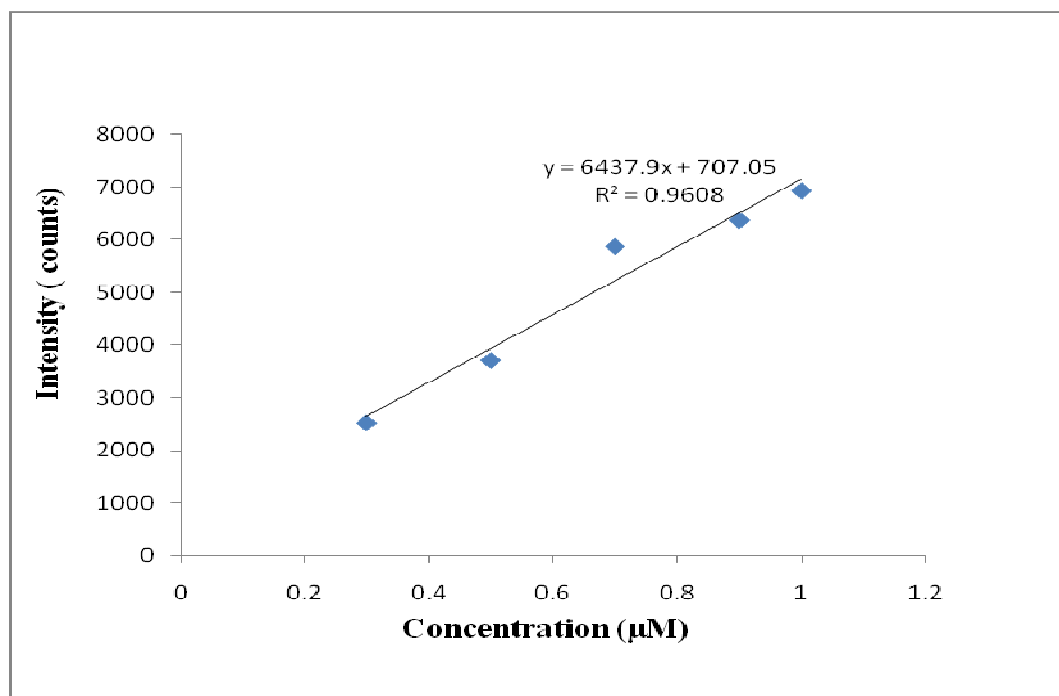


FIGURE 11 CALIBRATION CURVE OF RHODAMINE 6 G IN SILVER COLLOID

3.2.3 ABSORBANCE SPECTRA:

Absorbance measurements in the 650 nm to 900 nm range are an indication of the collective plasmon absorptions and can be used to evaluate the relative aggregations of

the metal nanoparticles in the sample solutions. Absorbance measurements were taken for different concentrations of R6G at 0 minutes and 5 minutes after sample preparation. These values were obtained at different wavelengths and graphs were plotted for absorbance values at wavelengths of 650 nm and 900 nm, respectively. The absorbance values taken at 650 nm and 900 nm were used to compare with the SERS enhancements. From the plot of the absorbance at 650 nm (figure 12), it was observed that there was an increase in the absorbance at approximately 50 μM at 5 minutes after the activator was added to the sample.

Concentration (μM)	0 mins	5 mins
0.1	1.3062	1.1067
0.5	1.3242	1.0851
1	1.2836	1.0941
5	1.2796	1.1072
10	1.2856	1.1291
50	1.2812	1.1375
100	1.3947	1.2265
500	1.4764	1.2996

TABLE 2 ABSORBANCE VALUES OF R6G AT 650 nm

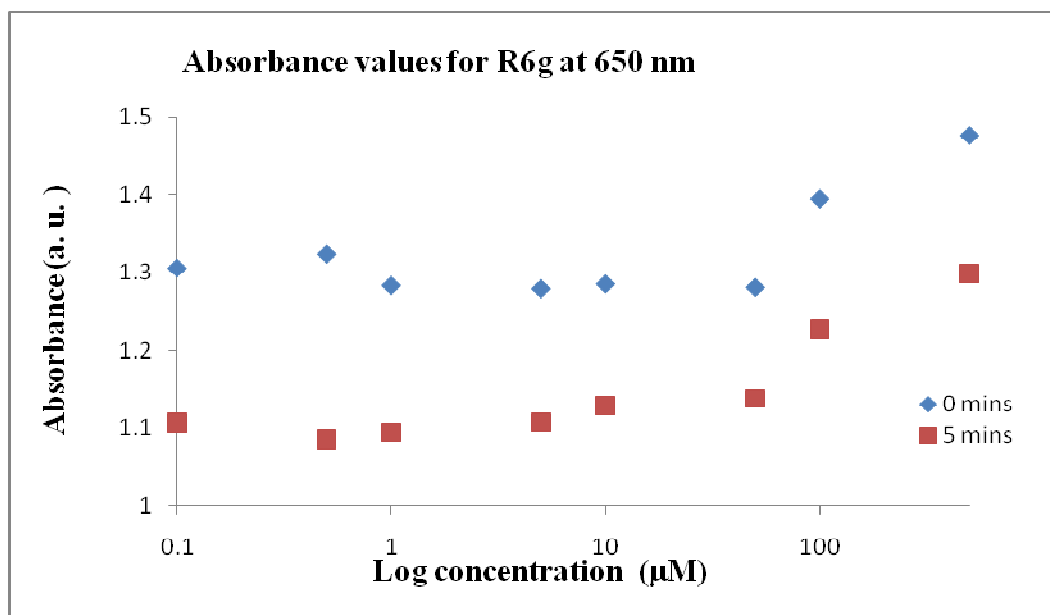


FIGURE 12 ABSORBANCE VALUES FOR R6G AT 650 nm

From the plot of the absorbance at 900 nm (Figure 13) at both 0 minutes and 5 minutes, it was observed that a slight increase occurred in the absorbance values at about 5 µM concentration of R6G at both 0 minutes and 5 minutes.

Concentration (µM)	0 mins	5 mins
0.1	1.6934	1.3806
0.5	1.6787	1.318
1	1.6857	1.3606
5	1.6728	1.4623
10	1.7275	1.5322
50	1.812	1.6494
100	1.8302	1.7302
500	1.8327	1.7045

TABLE 3 ABSORBANCE VALUES OF R6G AT 900 nm

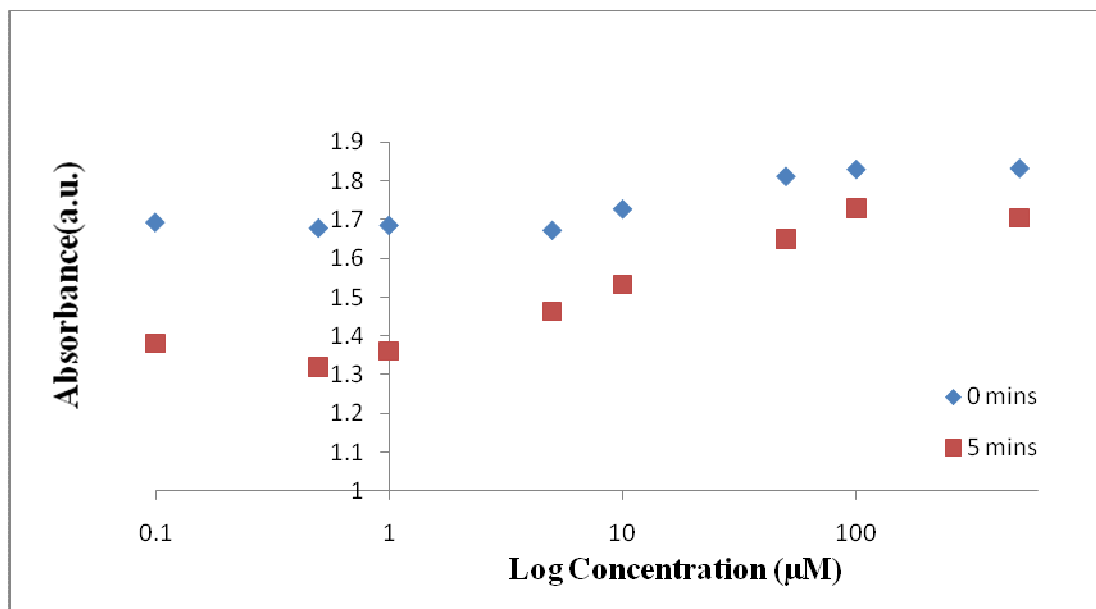


FIGURE 13 ABSORBANCE VALUES FOR R6G AT 900 nm

Shown in Table 4 and Figure 14 are the relative enhancement in the SERS response of R6G on silver nanoparticles. As the data show, the maximum enhancement is on the order of 1.5×10^5 and is highest at the lowest concentration (0.3 – 1 µM). As the concentration increases, the enhancement is observed to decrease and the threshold concentration is similar to that observed for the change in absorbance at 650 nm and 900 nm. The trend of these data is similar to that observed by Souza et al.²⁹ and suggests that the highest enhancements are associated with small aggregates of the silver nanoparticles.

Concentration (μM)	Enhancement
250	3073.8
100	3439.9
50	4257.6
10	14232.9
1	120413.7
0.9	133329.3
0.7	157988.8
0.5	139747.5
0.3	158499.8

TABLE 4: ENHANCEMENT VALUES OF R6G IN SILVER COLLOID AT DIFFERENT CONCENTRATIONS

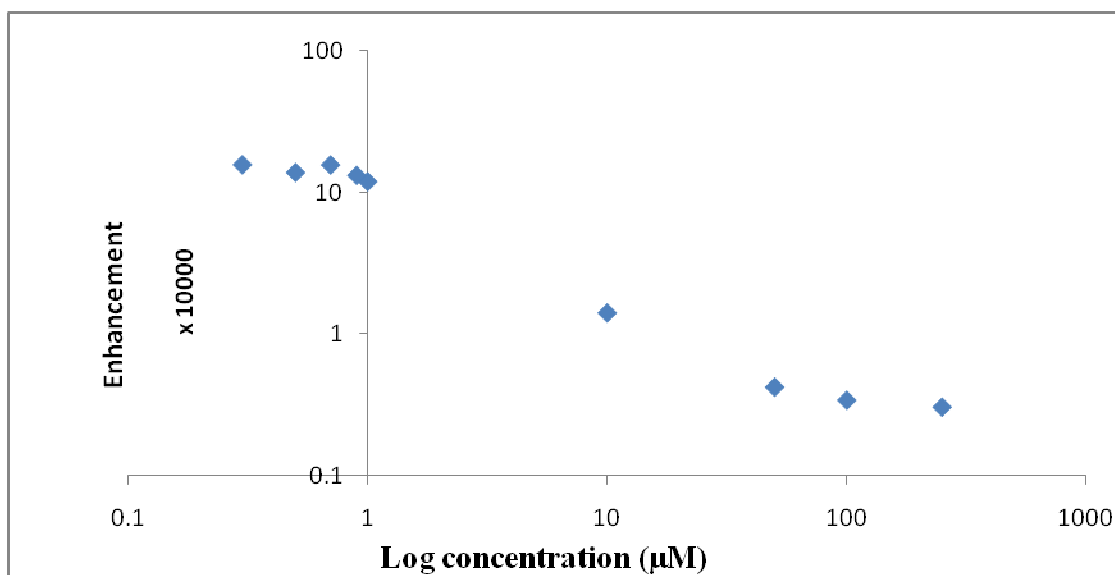


FIGURE 14 ENHANCEMENT EFFECT ON R6G WITH SILVER COLLOIDS

3.2.4 GOLD COLLOIDS:

SERS measurements of R6G in gold colloids were obtained in a similar way as that done with silver colloids. Data were obtained for different concentrations of R6G ranging from 100 μM to 0.1 μM at 0 minutes and 5 minutes. When compared to the data obtained with that of silver colloids, high SERS intensities were not obtained at lower concentrations of R6G.

3.3 CREATININE:

The SERS measurements for Creatinine were obtained in the presence of both silver and gold colloids at different integration times and at different time intervals. Several measurements were taken in order to determine the best linear responses and also to find the highest intensity. The measurements were taken for Creatinine at different concentrations such as 20 mM, 10 mM, 7 mM, 5 mM, 3 mM and 1 mM. With silver colloids, the maximum intensity was obtained at 0 minutes after activator addition. With gold colloids, the maximum intensity was obtained at 5 minutes after activator addition. An integration time of 10 sec was used for taking measurements with silver colloids and 60 sec integration time was used for taking the measurements with gold colloids. A 10 % NaCl solution was used as the activator in both cases. The quantities of the sample consisted of 2700 μL of silver / gold colloids + 300 μL of compound + 150 μL of activator. Creatinine stock solution was prepared by dissolving Creatinine compound in distilled water and the corresponding lower concentrations were prepared with distilled water. The highest intensities for Creatinine concentrations with silver colloids were obtained at wavenumbers 1411 cm^{-1} and 895 cm^{-1} and at wavenumbers 1437 cm^{-1} , 909

cm^{-1} , 699 cm^{-1} and 617 cm^{-1} with gold colloids. These values are in general agreement with those reported previously.³⁹

3.3.1 NORMAL RAMAN SPECTRA FOR CREATININE:

Figure 15 shows the normal Raman spectrum for Creatinine solution (20 mM) at 65 sec integration time. No activator or any colloid is added to the sample; only the sample solution is measured. The spectra in Figure 16 show the normal and SERS spectral features for different forms of Creatinine.

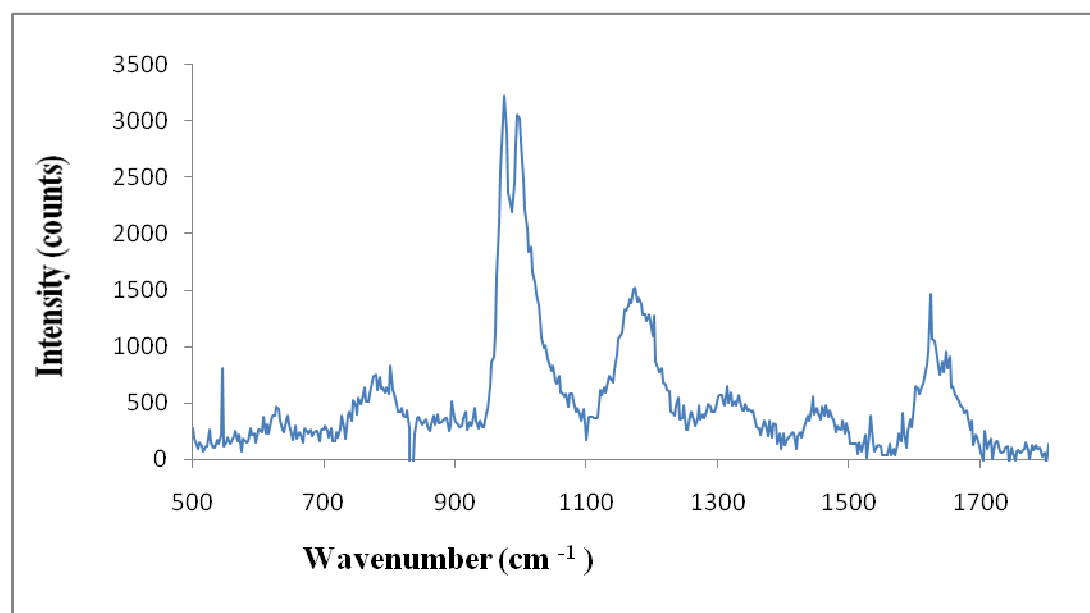


FIGURE 15 NORMAL RAMAN SPECTRA FOR CREATININE (20 mM) SOLUTION AT 65 SEC INTEGRATION TIME

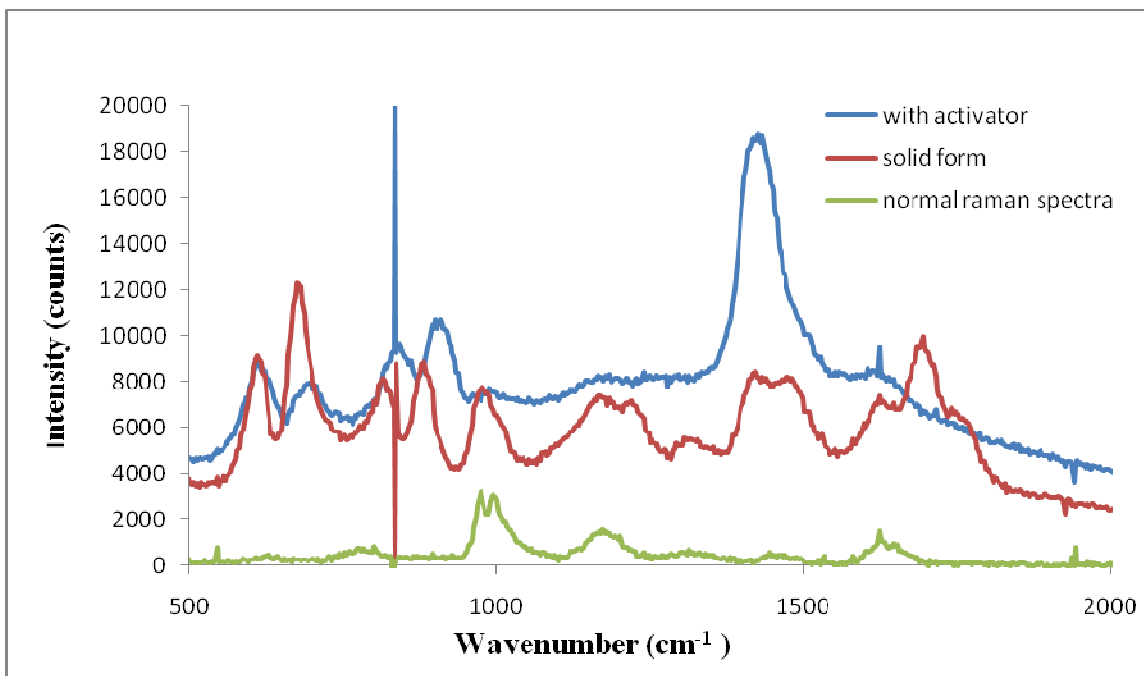


FIGURE 16 SPECTRA FOR CREATININE IN DIFFERENT FORMS

3.3.2 SILVER COLLOIDS:

SERS measurements were taken for different concentrations of Creatinine in the presence of silver colloids at 0 minutes and 5 minutes and an integration time of 10 sec was used. Concentrations ranging from 20 mM to 1mM were measured. From the graph shown in Figure 17, it was observed that there was linearity in the intensities with the increasing concentrations. The linearity was observed for the concentrations ranging from 3 mM to 20 mM. Maximum intensities were obtained at 0 minutes after activator addition to the sample. The highest intensities were obtained at 1411cm^{-1} and 895cm^{-1} , respectively.

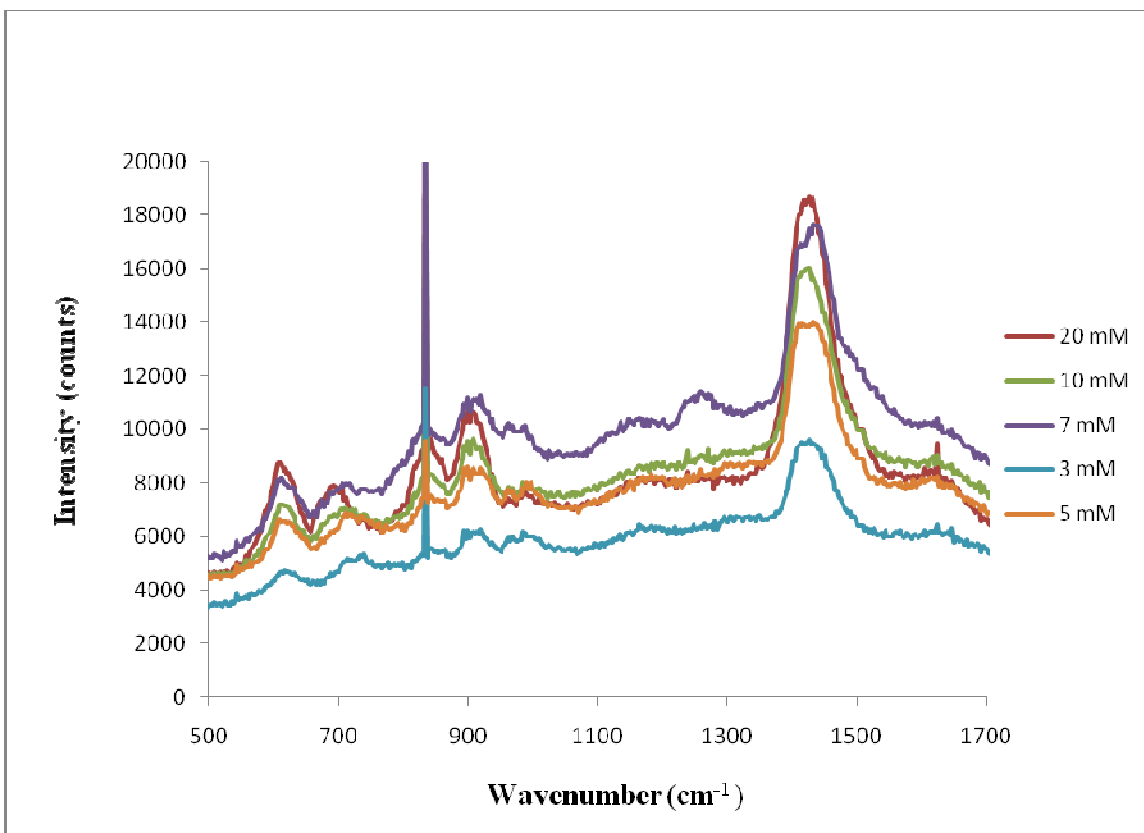


FIGURE 17 CREATININE SERS MEASUREMENTS AT 0 mins AT 10 sec INTEGRATION TIME

3.3.2.a CALIBRATION CURVE:

The calibration curve for SERS measurements of creatinine on silver (Ag) colloids is shown in Figure 18. From the SERS measurements at different concentrations, it is observed that linearity can be obtained from the concentrations ranging from 3 mM to 20 mM. These spectra were obtained at 0 minutes after the addition of the activator and at 10 sec integration time. The graph was plotted by considering the intensities at wavenumber 1141 cm^{-1} . The estimated LOD for creatinine on silver colloids is 2 mM.

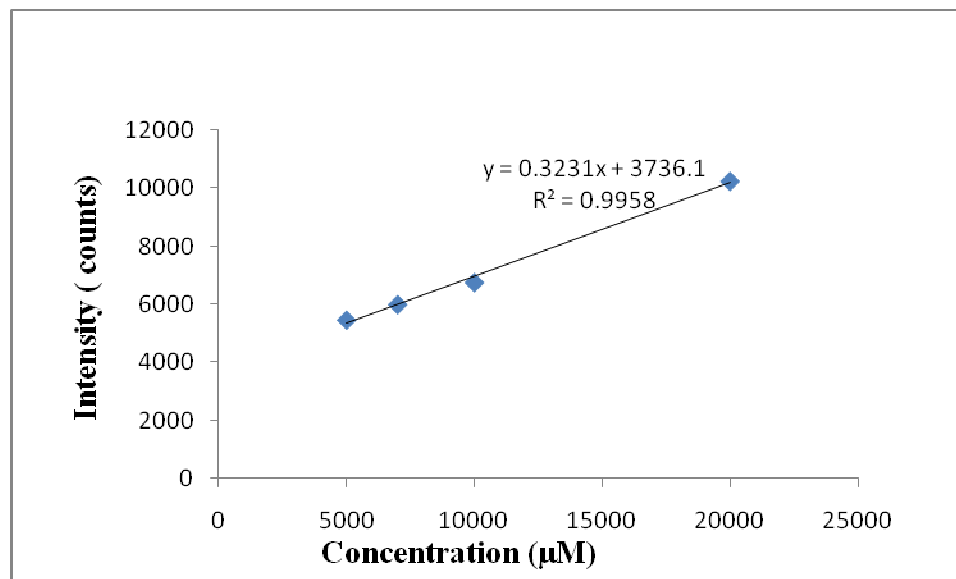


FIGURE 18 CALIBRATION CURVE OF CREATININE IN SILVER + NaCl AT 0 MINS AT 10 SEC INTEGRATION TIME

3.3.2.b ABSORBANCE SPECTRA AND ENHANCEMENT EFFECTS:

Absorbance data and SERS measurements were obtained for Creatinine in the presence of both silver and gold colloids, respectively. Absorbance spectra were taken for creatinine at different wavelengths at 0 minutes and 5 minutes after addition of the activator. The graphs shown below in Figures 19 and 20 were plotted for absorbance measurements at wavelengths 650 nm and 900 nm, by taking the concentrations on the X – axis and the absorbance values on the Y – axis.

From the absorbance data vs concentration graph plotted at 650 nm, it is seen that there is very little change in the absorbance values. The absorbances are observed to be relatively constant at both 0 minutes and 5 minutes after addition of the activator.

Concentration(μM)	0 mins	5 mins
20000	1.0912	0.0912
10000	1.1178	0.88218
7000	1.135	0.90403
5000	1.1347	0.86367
3000	1.1893	0.90031
1000	1.1595	0.82294

TABLE 5 ABSORBANCE VALUES OF CREATININE AT 650 nm

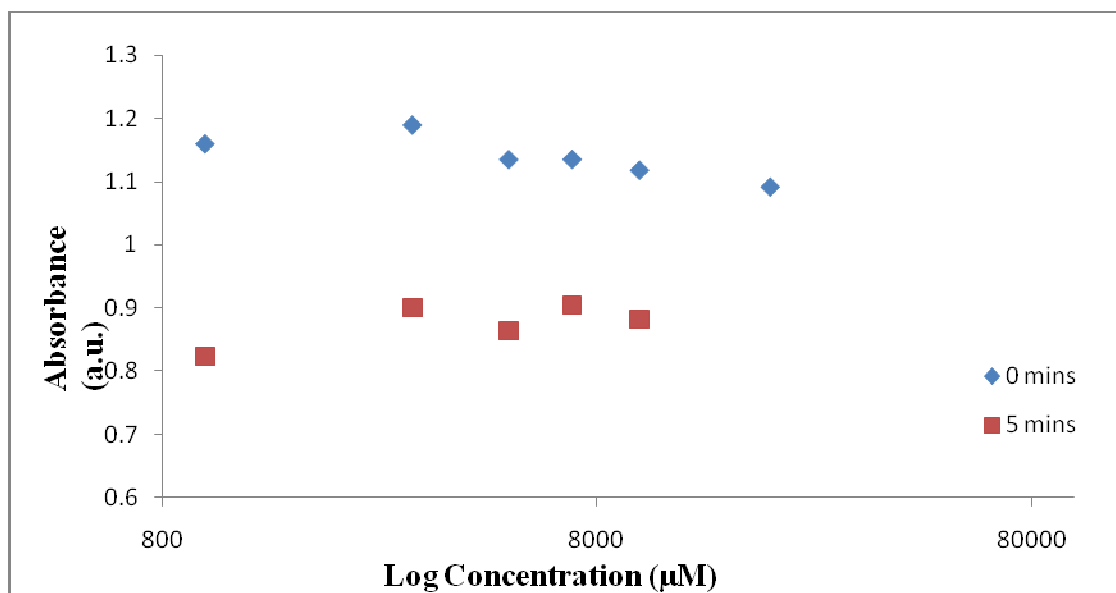


FIGURE 19 ABSORBANCE VALUES FOR CREATININE IN SILVER AT 650 nm

Concentration (μM)	0 mins	5 mins
20000	1.4875	1.0793
10000	1.4334	1.0077
7000	1.5098	0.95441
5000	1.4634	0.88351
3000	1.5568	0.93939
1000	1.3799	0.80305

TABLE 6 ABSORBANCE VALUES OF CREATININE AT 900 nm

The graph shown below is plotted by taking the absorbance values obtained at 0 minutes and 5 minutes at a wavelength of 900 nm on the Y- axis and the log concentrations on the X – axis. From the graph, it is observed that there is no significant change in the absorbance values at a concentration of 5 mM, both at 0 minutes and 5 minutes after activator addition to the sample.

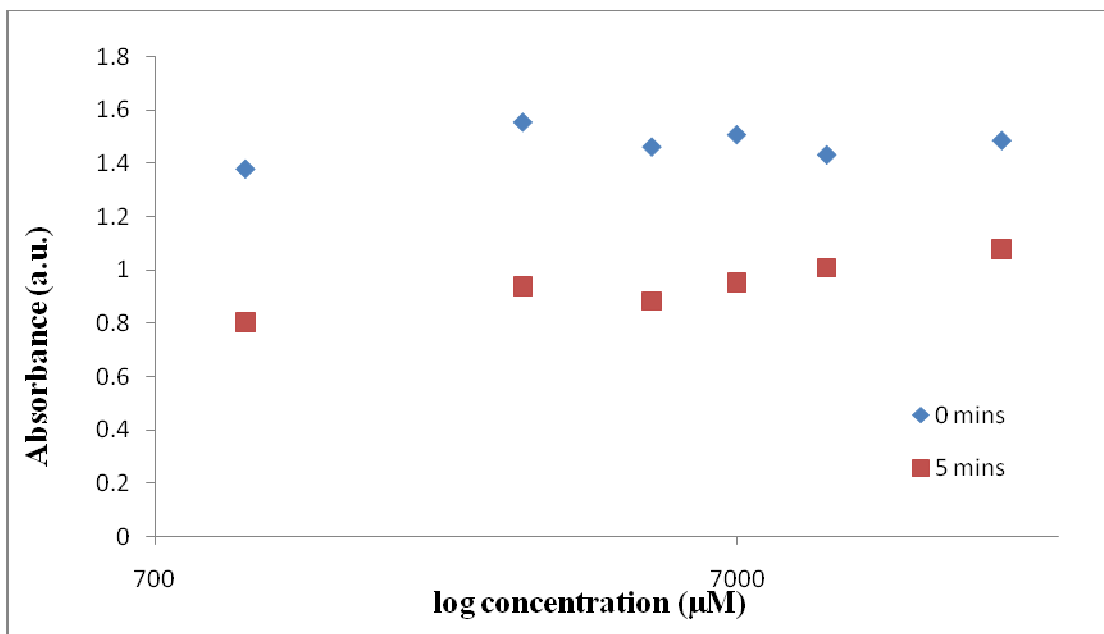


FIGURE 20 ABSORBANCE VALUES FOR CREATININE IN SILVER AT 900 nm

Show in Figure 21 are the relative enhancements for Creatinine on silver colloids. The enhancements are relatively small compared to the results observed for R6G on silver colloids and do not show a similar trend.

Concentration (µM)	Enhancement
1000	1002.051
3000	310.36
5000	136.692
7000	121.44
10000	66.128
20000	29.015

TABLE 7 ENHANCEMENT VALUES OF CREATININE IN GOLD COLLOIDS AT DIFFERENT CONCENTRATIONS

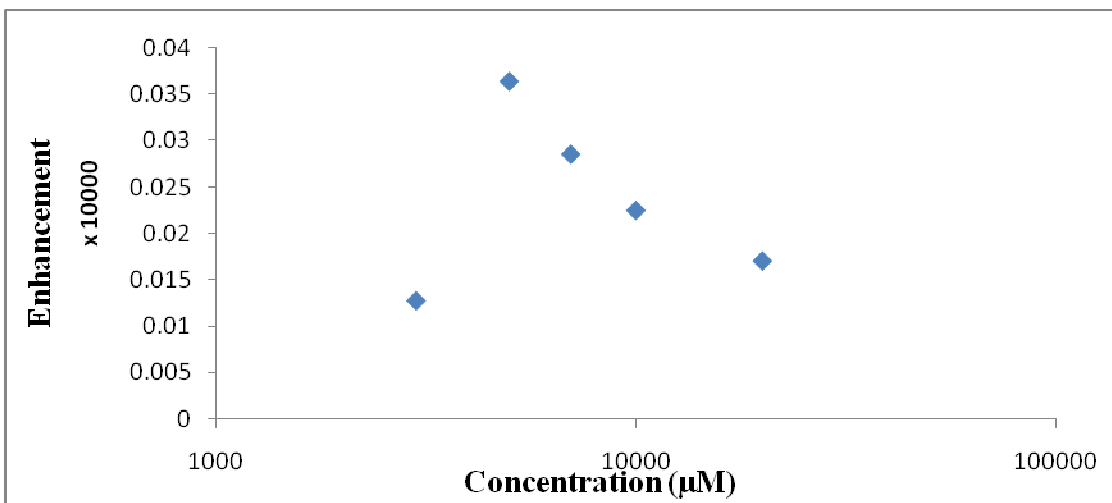


FIGURE 21 ENHANCEMENT EFFECT FOR CREATININE IN SILVER AT 0 mins

3.3.3 GOLD COLLOIDS:

SERS measurements were taken for Creatinine in the presence of gold colloids for different concentrations ranging from 1 mM to 20 mM at an integration time of 60 sec and at different intervals of time (0 minutes, 5 minutes). These spectra are shown in Figures 22 and 23. The maximum intensities for the concentrations were obtained at 5 minutes after activator addition to the sample. The intensities were seen to increase at wavenumbers 1437cm^{-1} , 909cm^{-1} , 699cm^{-1} and 617cm^{-1} respectively. Unlike SERS measurements in silver, no linearity was observed in the intensities of the concentrations of creatinine on gold colloids.

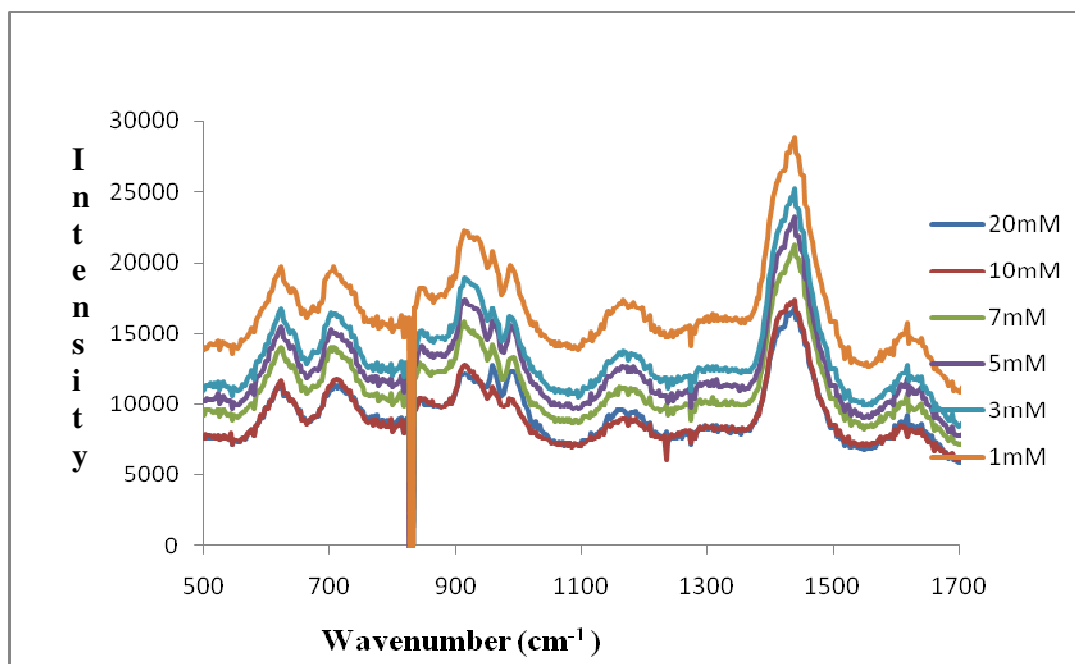


FIGURE 22 SERS SPECTRA FOR CREATININE AT 60 sec INTEGRATION TIME
AT 0 mins

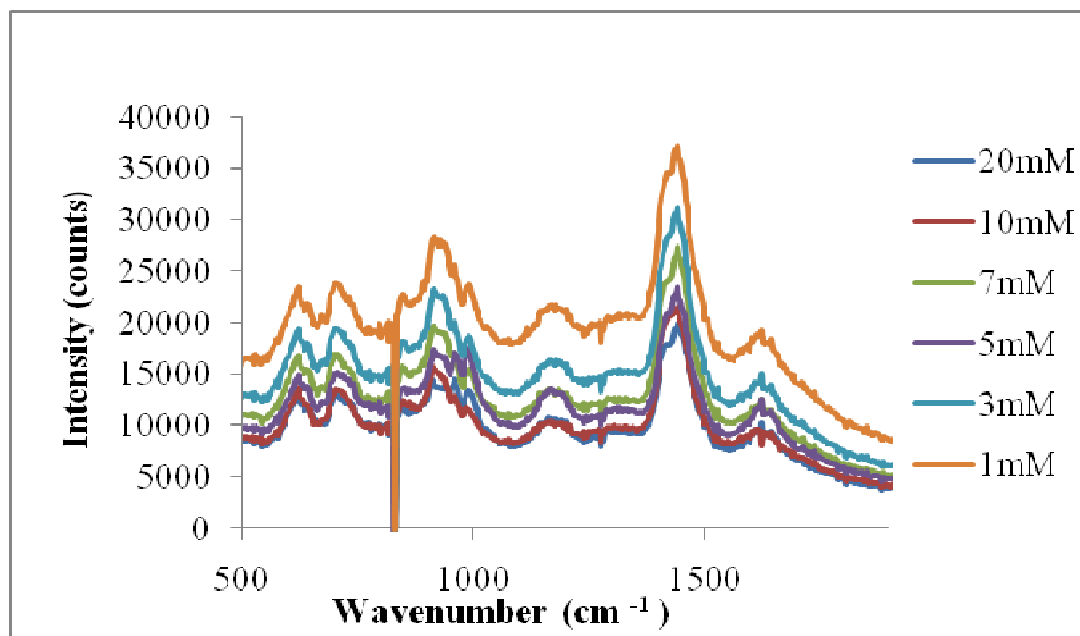


FIGURE 23 SERS SPECTRA FOR CREATININE AT 60 sec INTEGRATION TIME
AT 5 mins

3.3.3.a ABSORBANCE SPECTRA AND ENHANCEMENTS EFFECTS FOR CREATININE WITH GOLD COLLOIDS:

Absorbance spectra were taken for different concentrations of creatinine in the presence of gold colloids. The data were obtained at different wavelengths and at different intervals of time (0 mins and 5 mins). Spectra were obtained for different concentrations ranging from 1 mM to 20 mM. Graphs were plotted by considering the absorbance values obtained at 0 mins and 5 mins at 650 nm and 900 nm wavelengths.

Concentration (μM)	0 mins	5 mins
20000	0.61332	0.52922
10000	0.57328	0.50124
7000	0.54111	0.46842
5000	0.53735	0.46914
3000	0.50132	0.43407
1000	0.56978	0.48769

TABLE 8 ABSORBANCE VALUES OF CREATININE WITH GOLD COLLOIDS AT 650 nm

From the data in Figure 24, it is seen that the absorbance values obtained at 650 nm wavelength are relatively constant over this concentration range.

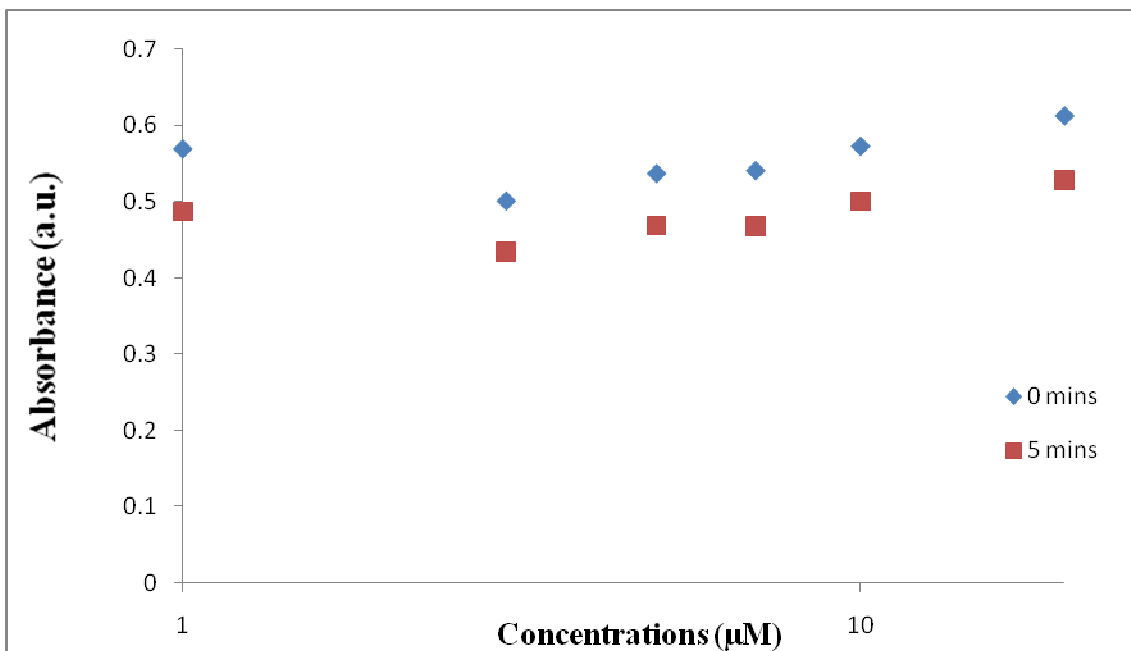


FIGURE 24 ABSORBANCE VALUES FOR CREATININE IN GOLD AT 650 nm

At 900 nm wavelength, it is observed that the absorbance values are relatively constant at both 0 mins and 5 mins. The data in Table 9 show the values obtained at 900 nm at 0 mins and 5 mins. As Figure 25 shows, the absorbance values of creatinine on gold colloids are relatively constant at this wavelength.

Concentration (μM)	0 mins	5 mins
20000	0.14021	0.27163
10000	0.13973	0.26781
7000	0.1206	0.24884
5000	0.13156	0.26535
3000	0.09832	0.2295
1000	0.13329	0.30716

TABLE 9 ABSORBANCE VALUES OF CREATININE WITH GOLD COLLOID AT
900 nm

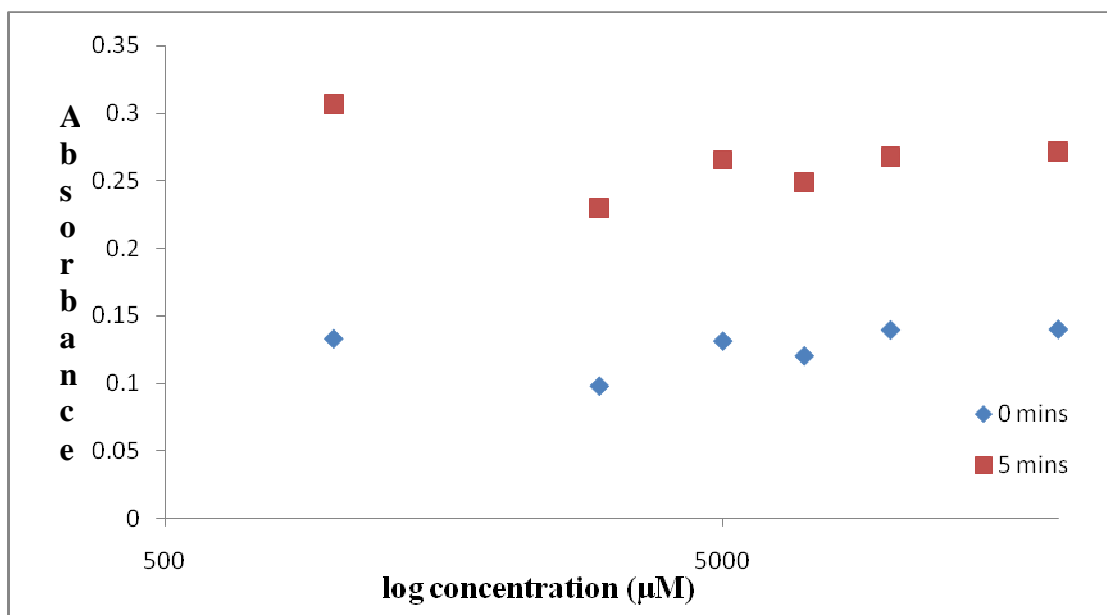


FIGURE 25 ABSORBANCE VALUES OF CREATININE WITH GOLD COLLOID AT
900 nm

Shown in Figure 26 is the relative enhancement for creatinine on gold colloids. The enhancements are relatively small compared to those observed for R6G on silver and do not show a similar trend.

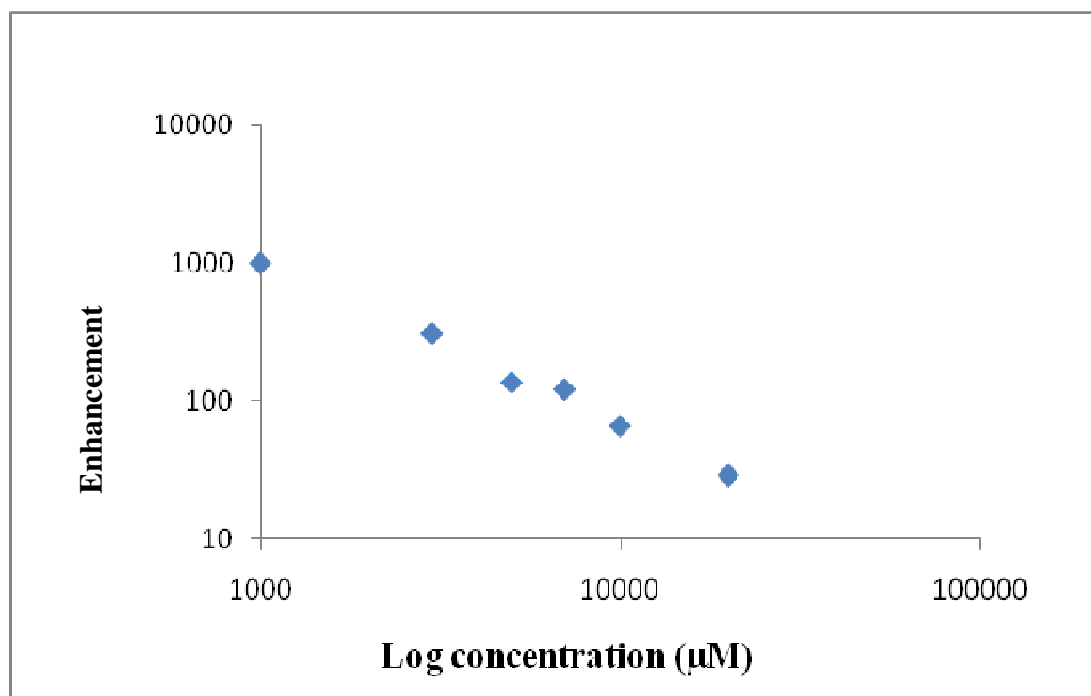


FIGURE 26 ENHANCEMENT EFFECT OF CREATININE IN GOLD COLLOIDS

3.4 IMIDAZOLE:

SERS measurements for imidazole were taken by measuring different concentrations of imidazole ranging from 1 mM to 20 mM. The readings were taken at different intervals of time (0 minutes and 5 minutes) and at different integration times (10 sec, 30 sec, and 60 sec) to find the best linearity and highest sensitivity. The stock solutions of imidazole were prepared by dissolving imidazole (solid form) in distilled

water. The series of dilutions were prepared by diluting with distilled water. Maximum intensity values were obtained at 10 sec integration time at 0 minutes after activator addition to the sample in the presence of silver colloids, and at 30 sec integration time in the presence of gold colloids. The intensities varied with the change in the integration time and time intervals after sample preparation. A 10% NaCl solution was used as the activator for obtaining all measurements. The sample consisted of (2700 μL of silver / gold colloids + 300 μL of sample being measured + 150 μL of activator).

The highest intensities for imidazole were obtained at wavenumbers (1140.9 cm^{-1} and 1234.9 cm^{-1} , 1311.8 cm^{-1}) with silver colloids and at almost the same wavenumbers (1143.7 cm^{-1} , 1237.7 cm^{-1} , 1323.2 cm^{-1}) with gold colloids. These Raman shift values are in general agreement with those reported previously.²⁹

3.4.1 NORMAL RAMAN SPECTRA OF IMIDAZOLE:

Figure 27 represents the normal Raman spectra for imidazole at 65 sec integration time. The sample taken for measuring the normal Raman spectra consisted of 2g/100ml of imidazole dissolved in distilled water. Several measurements of distilled water were taken at the same integration time and the average spectrum was subtracted from the normal Raman spectrum of imidazole. All Raman and SERS measurements were background subtracted.

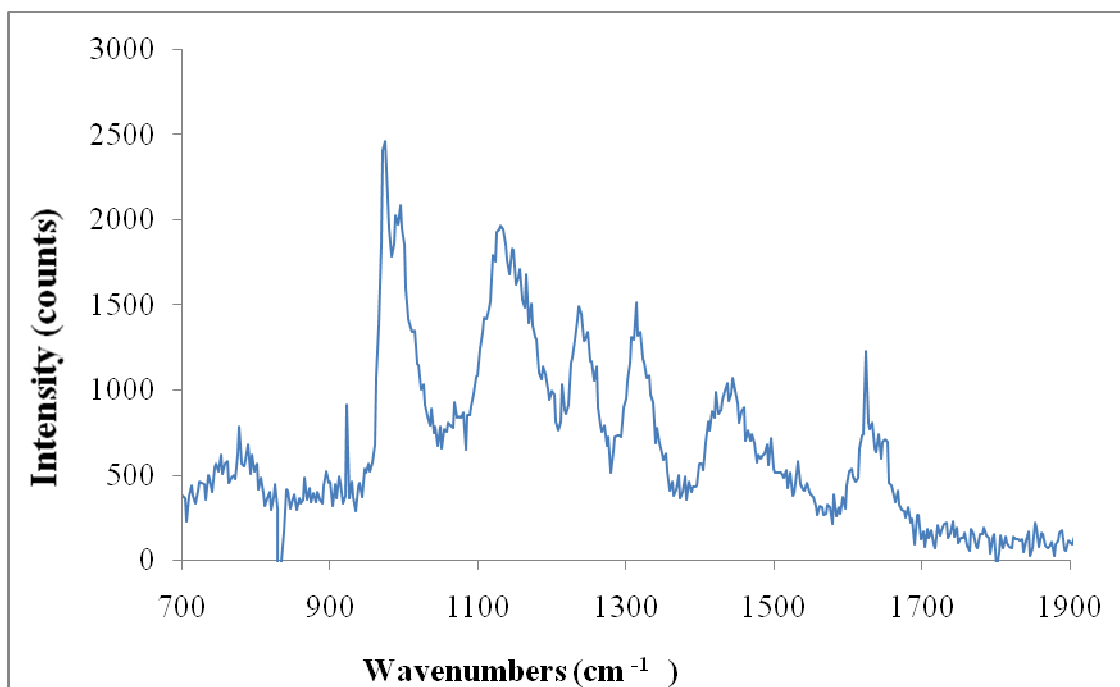


FIGURE 27 NORMAL RAMAN SPECTRA FOR IMIDAZOLE

The spectra in Figure 28 show the different forms of imidazole compound (normal Raman spectrum, SERS spectrum for imidazole with an activator and spectrum for solid form for imidazole).

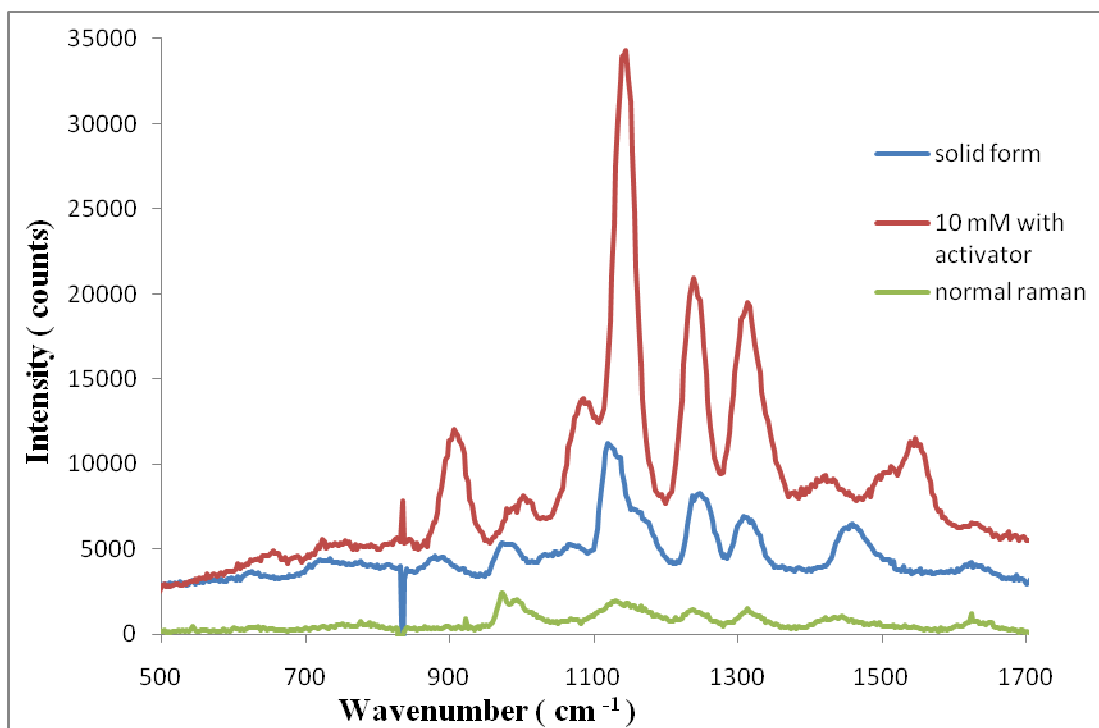


FIGURE 28 SPECTRA FOR DIFFERENT FORMS OF IMIDAZOLE

3.4.2 SILVER COLLOIDS:

SERS spectra were obtained for imidazole in the presence of silver colloids at different concentrations ranging from 1 mM to 20 mM. Highest intensities were obtained at 0 minutes after activator addition to the sample and at an integration time of 10 sec. Maximum intensities were obtained at 1140.9 cm^{-1} and 1234.9 cm^{-1} and 1311.8 cm^{-1} wavenumbers, respectively. From the results in Figure 29, it is seen that the intensities increase linearly with the increase in the concentrations of imidazole, so linearity can be achieved from 1 mM to 20 mM concentration range.

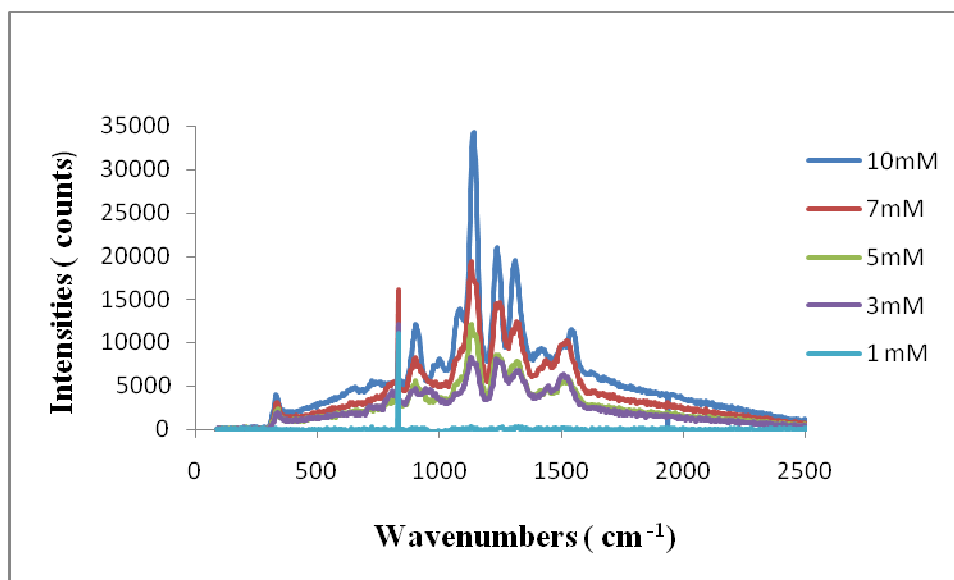


FIGURE 29 SERS SPECTRA OF IMIDAZOLE AT 10 sec AT 0 mins

3.4.2.a CALIBRATION CURVES:

It was observed that linearity can be achieved from the concentrations of imidazole ranging from 1 mM to 20 mM. The maximum intensities were obtained at 0 minutes at 10 sec integration time. The calibration curve in figure 30 was drawn by taking the intensities obtained at wave number 1140.9 cm^{-1} . A slope of 3083.6 and a y – intercept value of 6026.2 were determined from the calibration curve data.

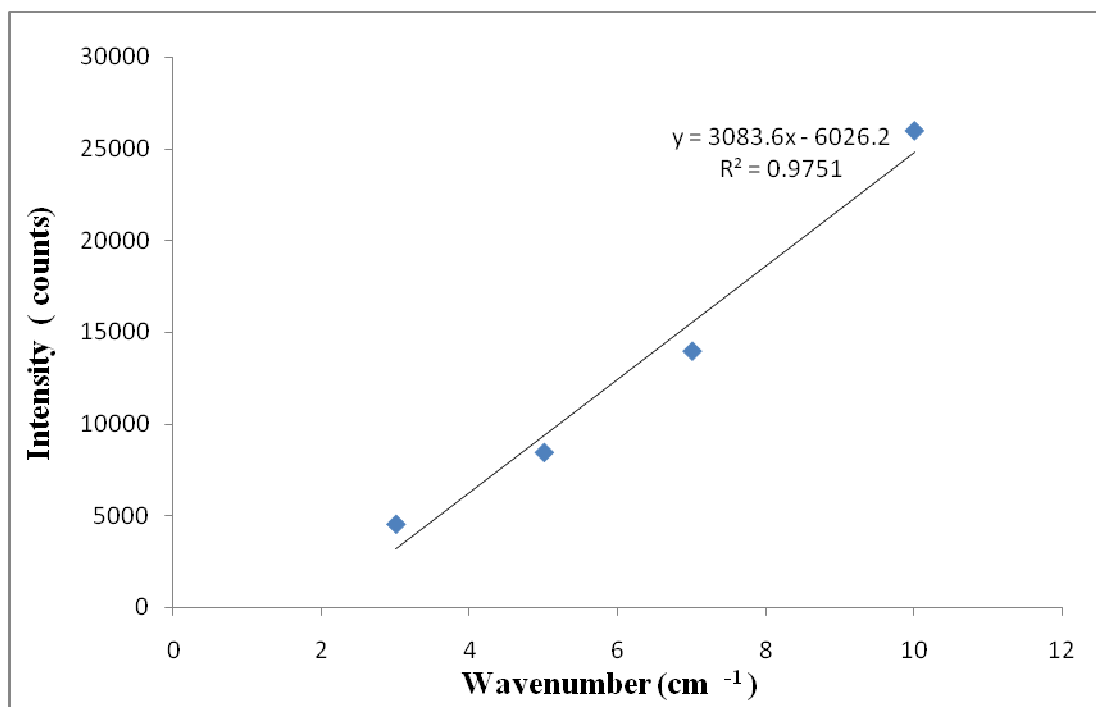


FIGURE 30 CALIBRATION CURVE FOR IMIDAZOLE AT 1138 cm^{-1} AT 10 sec
INTEGRATION TIME AT 0 mins

The calibration curve in Figure 31 was plotted by taking the intensities obtained at wavenumber 1234.9 cm^{-1} . A slope of 1101.9 and a y – intercept value of 669.57 were calculated from the calibration curve. The linearity and correlation is not good at this Raman shift as the results at 1138 cm^{-1} .

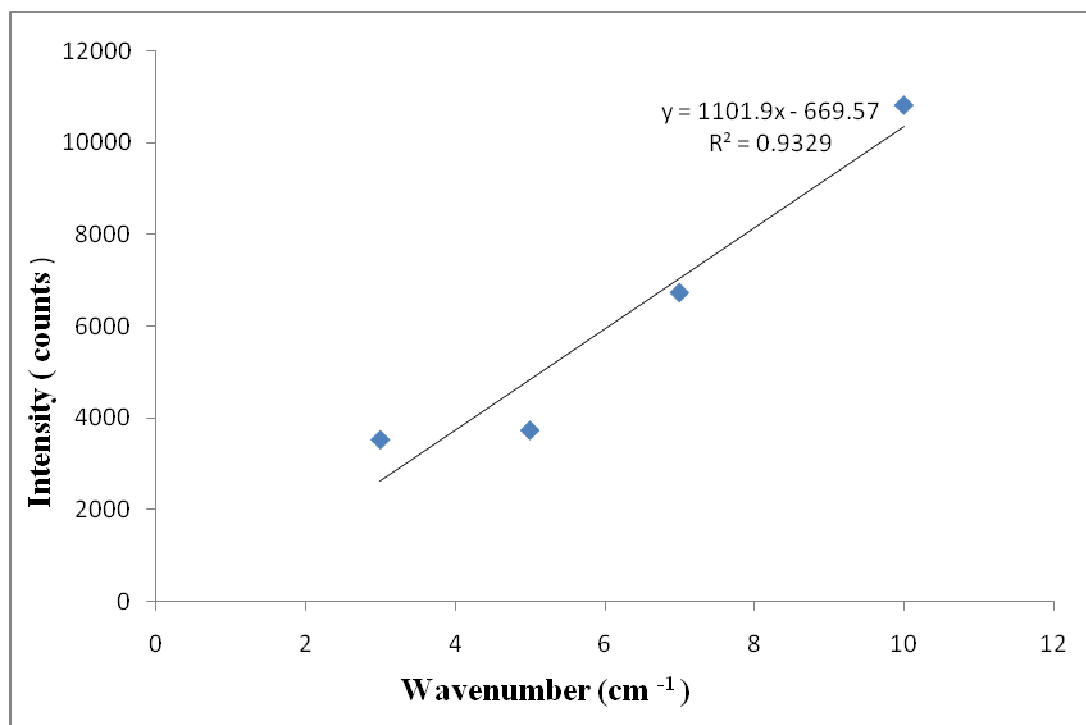


FIGURE 31 CALIBRATION CURVE FOR IMIDAZOLE 1234.9 cm⁻¹ AT 10 sec INTEGRATION TIME AT 0 mins

3.4.2.b ABSORBANCE SPECTRA AND ENHANCEMENTS EFFECTS:

Both SERS measurements and absorbance spectra were taken at the same concentrations of imidazole. Absorbance spectra were obtained at different wavelengths for different concentrations ranging from 1 mM to 10 mM. The measurements were taken at 0 minutes and 5 minutes after activator addition to the sample. Graphs were plotted by taking the absorbance values in table 10 that were obtained at 650 nm and 900 nm wavelengths at both 0 minutes and 5 minutes time intervals. It is seen in Figure 33 that the absorbance values are relatively constant for imidazole at 650 nm at 0 minutes and 5 minutes.

Concentration (μM)	0 mins	5 mins
10000	1.104	0.88138
7000	1.1859	0.93651
5000	1.1098	0.84856
3000	1.1559	0.86927
1000	1.1955	0.89415

TABLE 10 ABSORBANCE VALUES OF IMIDAZOLE IN SILVER COLLOIDS AT
650 nm

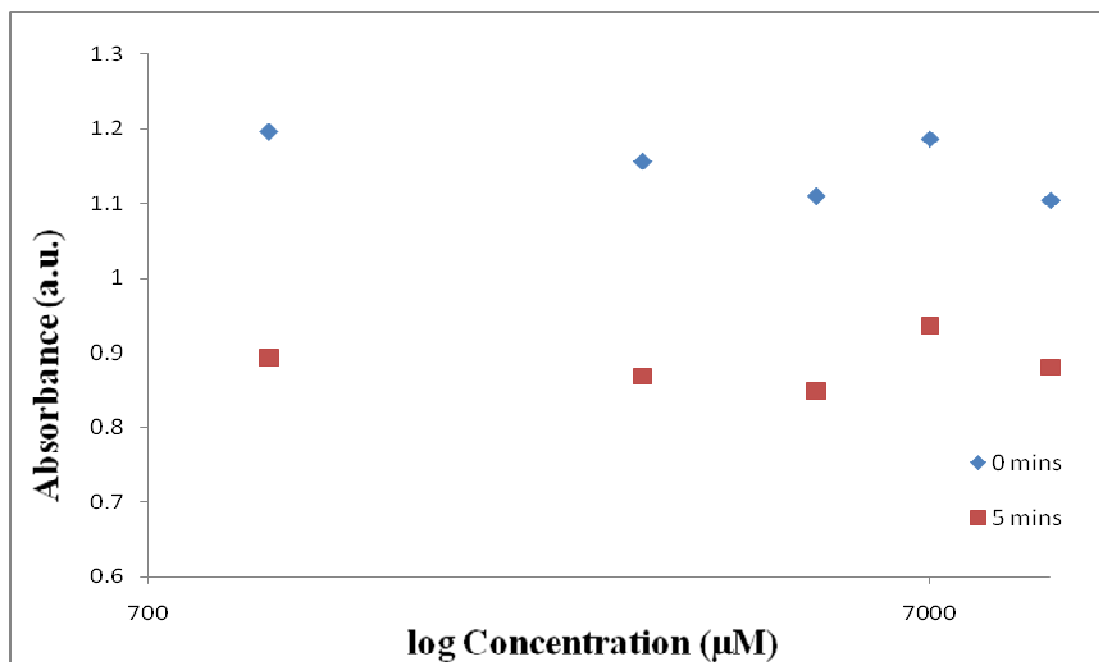


FIGURE 32 ABSORBANCE VALUES FOR IMIDAZOLE IN SILVER COLLOID AT
650 nm

Similar results were observed at 900 nm wavelength (shown in Figure 33) where there is no significant change in the absorbance values at 0 minutes, or at 5 minutes time interval (Table 11).

Concentration (μM)	0 mins	5 mins
10000	1.4324	1.0033
7000	1.4979	1.079
5000	1.495	0.89472
3000	1.4573	0.88187
1000	1.5166	0.98568

TABLE 11 ABSORBANCE VALUES OF IMIDAZOLE WITH SILVER COLLOID AT 900 nm

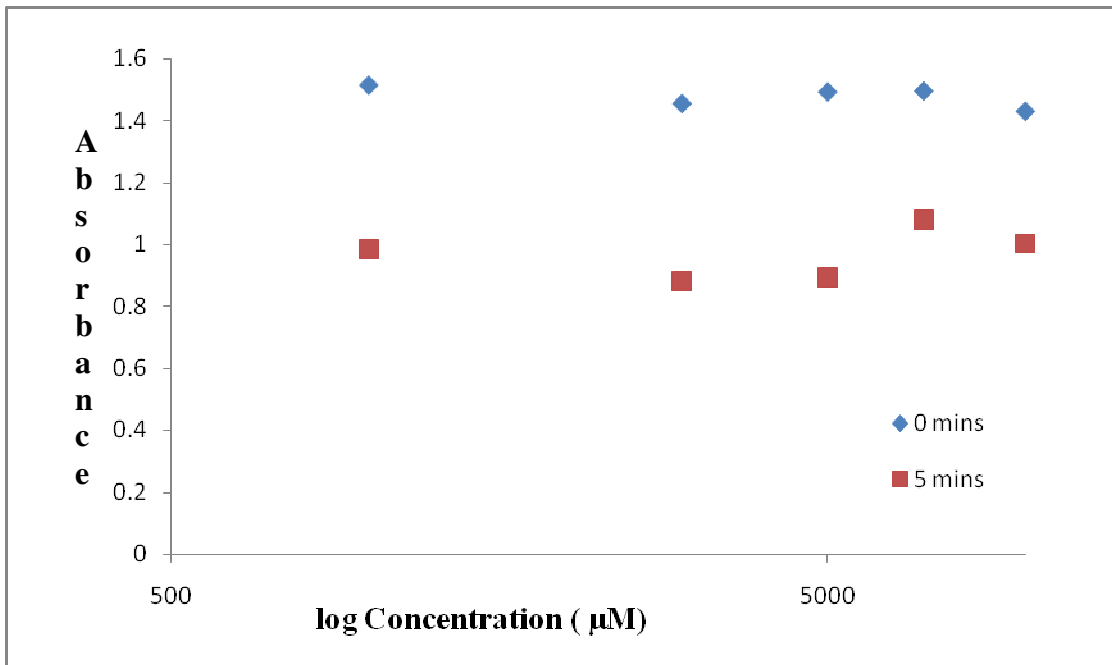


FIGURE 33 ABSORBANCE VALUES FOR IMIDAZOLE IN SILVER COLLOID AT 900 nm

From the enhancement vs concentration graph it is seen that there may be a small increase in the enhancement with increasing concentration of imidazole (Figure 34).

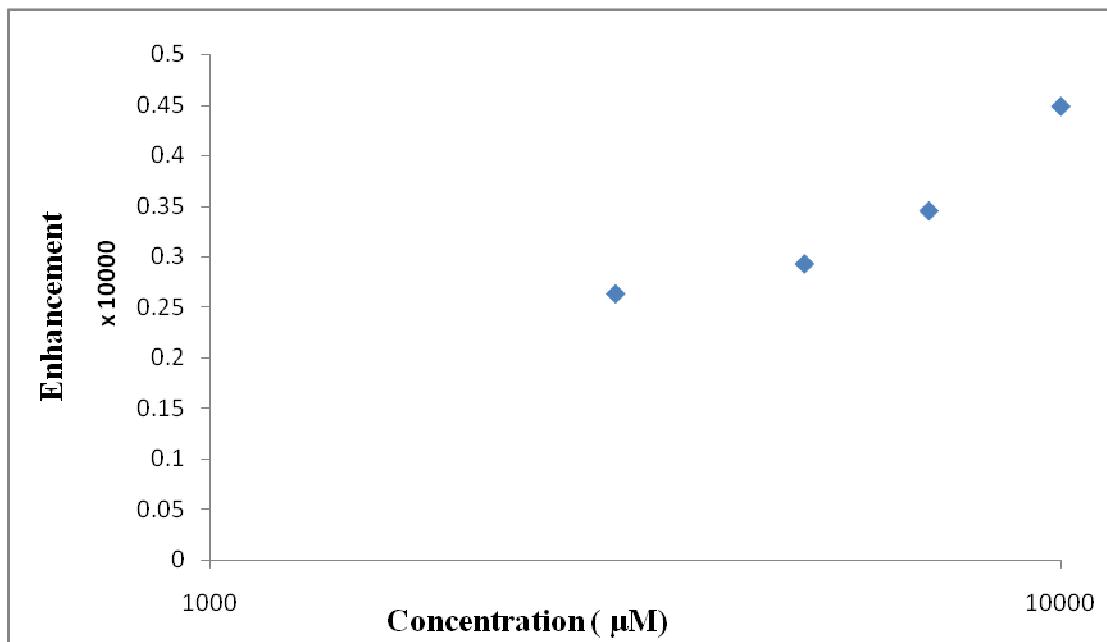


FIGURE 34 IMIDAZOLE PEAK 1138 cm^{-1}

For the enhancement values obtained at 1234.9 cm^{-1} (intensity values), it is seen that there are relatively constant enhancements over this concentration range. The enhancements observed for imidazole on silver colloids are low compared to those reported previously for imidazole on gold nanoparticles by Souza et al.²⁹

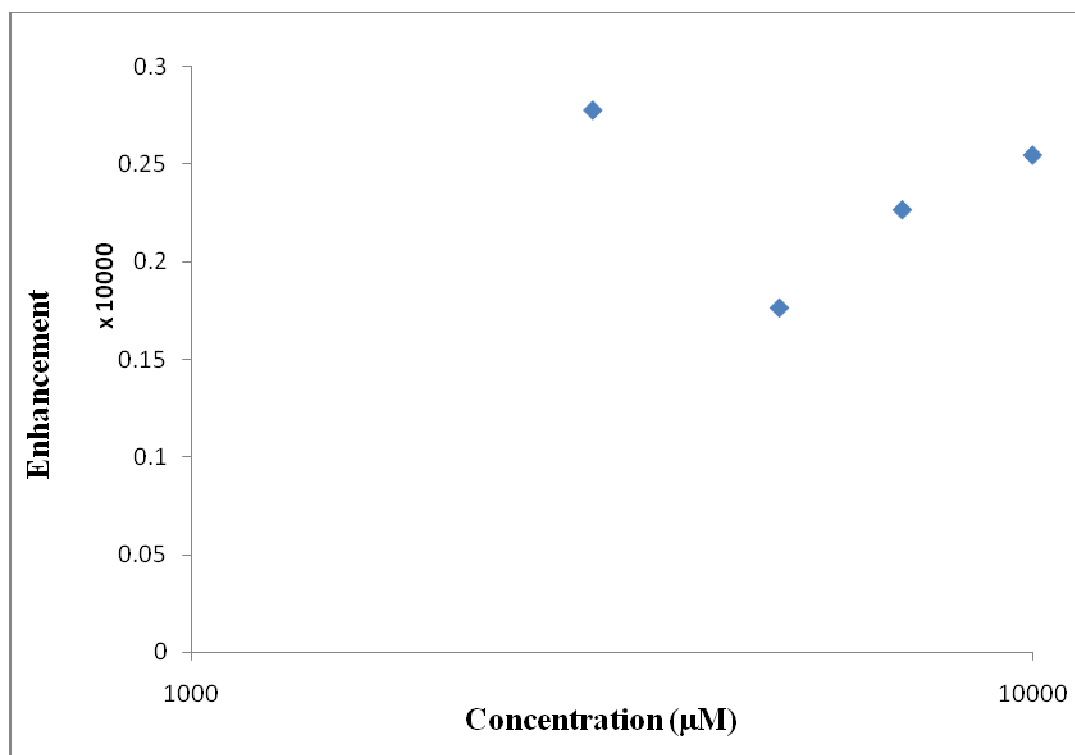


FIGURE 35 IMIDAZOLE PEAKS 1234.88 cm^{-1}

3.4.3 GOLD COLLOIDS:

SERS measurements were taken for imidazole in the presence of gold colloids. Different concentrations of imidazole were measured at an integration time of 30 sec and at 0 minutes and 5 minutes time intervals. High SERS intensities were obtained at 0 minutes after activator addition to the sample solution. Concentrations ranging from 1 mM to 10 mM were used for taking the measurements. The maximum intensities were obtained at 1143.7 cm^{-1} , 1237.7 cm^{-1} and 1323.2 cm^{-1} wavenumbers, respectively. The sample consisted of 2700 μL of gold colloid + 300 μL of compound being measured + 150 μL of activator. A 10 % NaCl solution was used as the activator for all concentrations. The graph in Figure 36 showed an increase in intensities with an increase

in the concentrations. However, the increase in intensities was not linear. The reason for this nonlinearity is not known at this time.

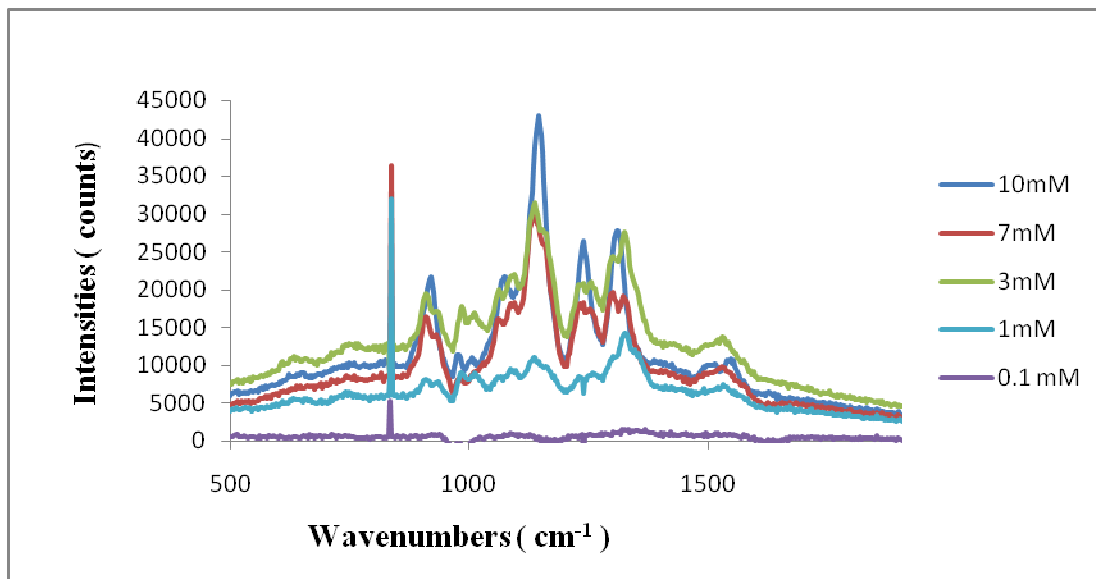


FIGURE 36 SERS MEASUREMENTS FOR IMIDAZOLE AT 0 mins AT 30 sec INTEGRATION TIME

3.4.3. a ABSORBANCE SPECTRA AND ENHANCEMENT EFFECTS FOR IMIDAZOLE IN GOLD COLLOIDS:

Absorbance spectra were obtained for different concentrations of imidazole ranging from 1 mM to 10 mM concentrations, at different wavelengths and at different intervals of time (0 mins, 5 mins). Graphs were plotted by considering the absorbance values obtained at 650 nm and 900 nm wavelengths (Figures 37 and 38). The log concentration values were taken on the X- axis and the absorbance values were taken on the Y – axis. The data in Table 12 below shows the values obtained at both 0 mins and 5 mins intervals of time at 650 nm wavelength.

Concentration (μM)	0 mins	5 mins
10000	0.44842	0.40678
7000	0.46106	0.42375
5000	0.39723	0.34892
3000	0.4691	0.42787
1000	0.59785	0.5043

TABLE 12 ABSORBANCE VALUES OF IMIDAZOLE WITH GOLD COLLOIDS AT
650 nm

From Figure 38, it is seen that the absorbance values are relatively constant over this range of imidazole concentrations at both 0 mins and 5 mins intervals of time.

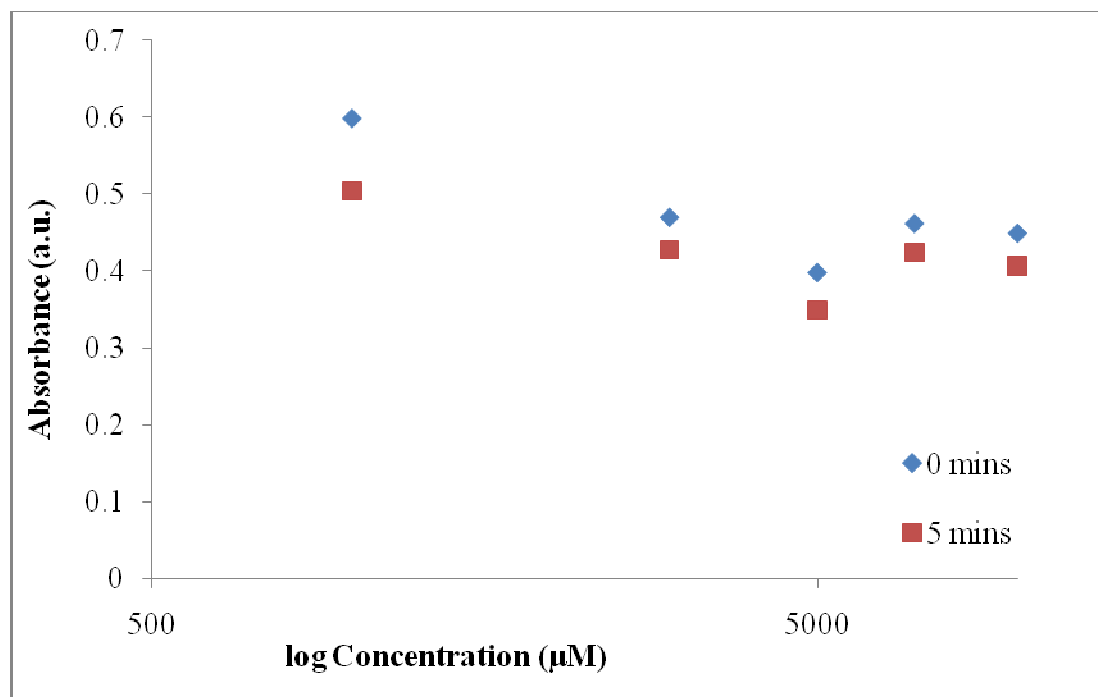


FIGURE 37 ABSORBANCE VALUES FOR IMIDAZOLE in gold colloid AT 650 nm

Table 13 shows the absorbance values obtained at both 0 mins and 5 mins at 900 nm wavelength. From the graph in Figure 39 for absorbance vs log concentrations at 900 nm, it is observed that the absorbance values are relatively constant at 0 mins and 5 mins intervals of time. These results are different from those reported previously by Souza et al.²⁹ They are also different from similar data obtained for R6G on silver colloids obtained in this same study.

Concentration (μM)	0 mins	5 mins
10000	0.18951	0.33439
7000	0.20335	0.3493
5000	0.11015	0.2606
3000	0.20802	0.36405
1000	0.1621	0.37536

TABLE 13: ABSORBANCE VALUES OF IMIDAZOLE IN GOLD COLLOIDS AT
900 nm

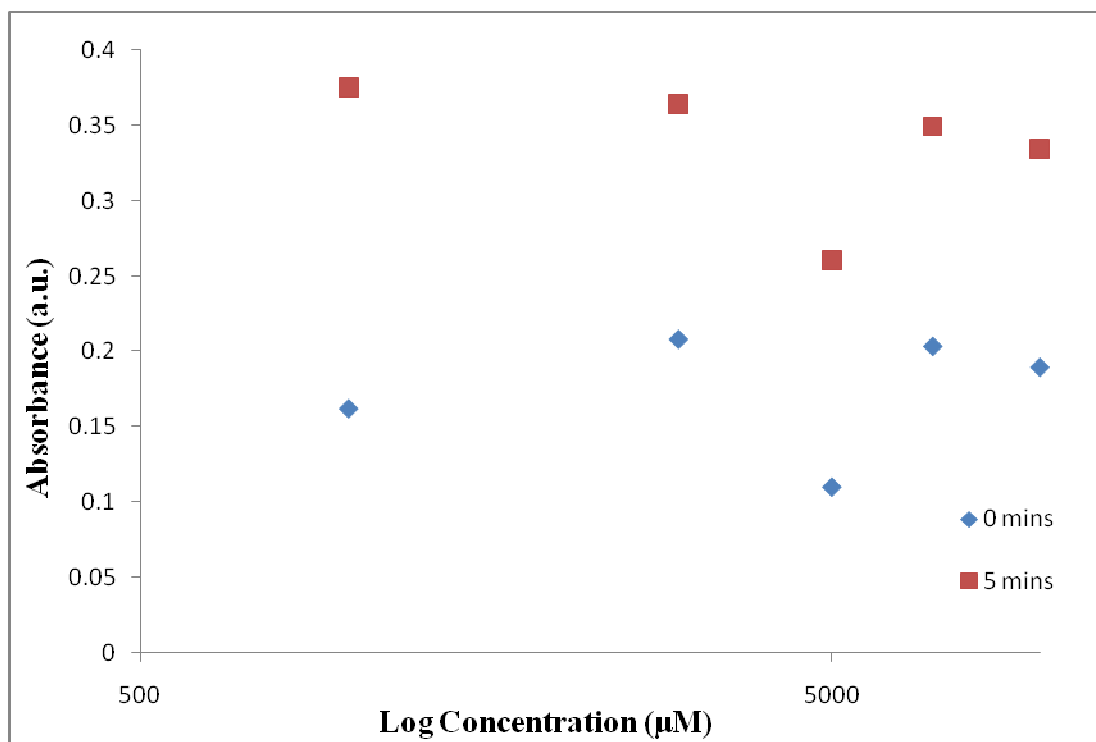


FIGURE 38 ABSORBANCE VALUES FOR IMIDAZOLE IN GOLD COLLOID AT
900 nm

For the calculated enhancement values obtained at peak 1(1138cm⁻¹), it is observed that there is no obvious trend in the enhancement factor (Figure 39). In the case of the graph drawn from peak 2(1234.8 cm⁻¹), there is no obvious trend in the enhancement (Figure 40). However, more measurements should be performed to confirm these results.

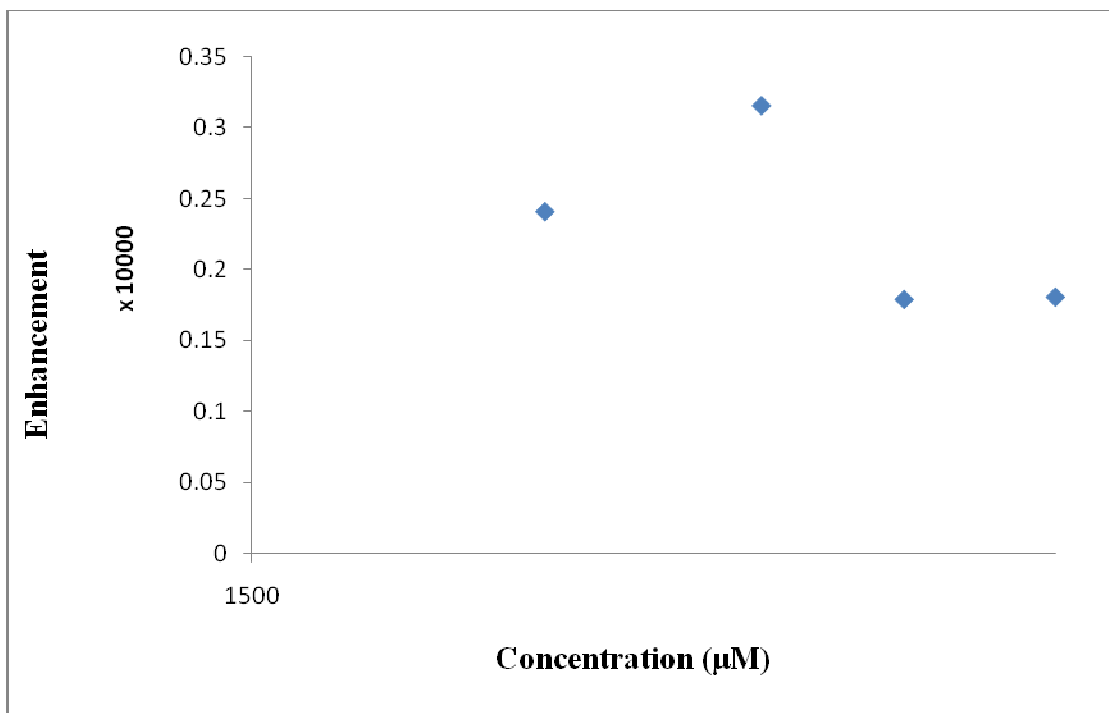


FIGURE 39 IMIDAZOLE PEAK 1138 cm⁻¹

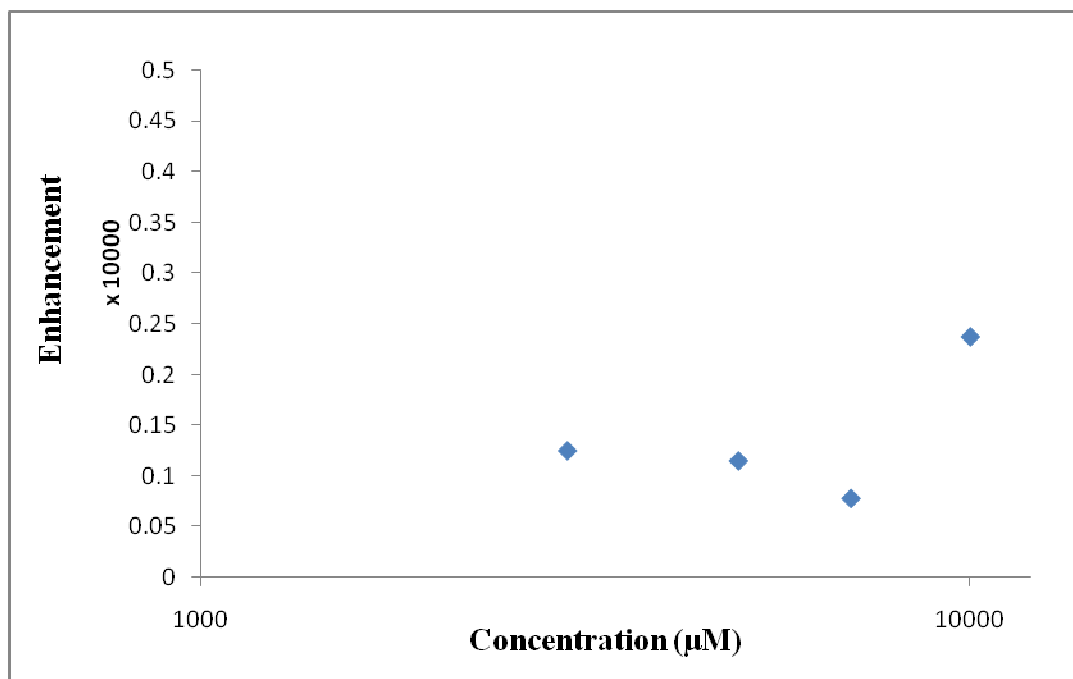


FIGURE 40 IMIDAZOLE PEAK 1234.883cm⁻¹

3.5 BENZOIC ACID:

A visible laser was used for taking SERS measurements of benzoic acid on silver colloids. Measurements were performed for benzoic acid in order to obtain the highest intensity and to check the reproducibility of the data taken. A 5 % NaNO_3 solution was used as the activator for taking measurements for benzoic acid. An integration time of 120 sec was used to obtain the SERS spectra (Figure 41). The measurements were taken at different intervals of time (0 mins, 5 mins). The maximum intensity was obtained at 0 mins after activator addition to sample. The intensities for benzoic acid were observed in the presence of silver colloids. Different concentrations of benzoic acid were measured for studying the linear responses of the intensities with respect to the concentrations being measured. Concentrations ranging from 1 mM to 100 mM were measured. The sample consisted of 2700 μL of silver colloid/ + 300 μL of compound being measured + 150 μL of activator (5% NaNO_3). The maximum intensities for benzoic acid were obtained at 952.7825 cm^{-1} , 1163.6455 cm^{-1} , 1964.355 cm^{-1} and 2163.82 cm^{-1} wavenumbers. No linearity was observed for benzoic acid measurements over this concentration range.

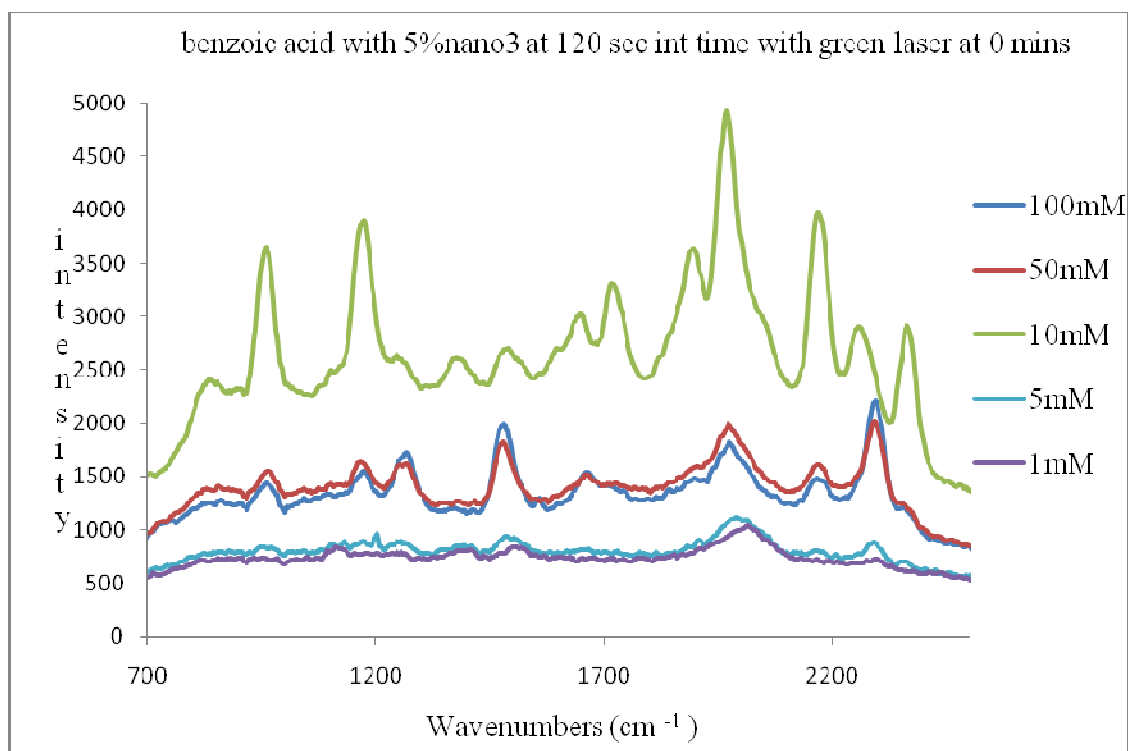


FIGURE 41 BENZOIC ACID WITH 5% NaNO₃ AT 120 sec INTEGRATION TIME AT 0 mins

3.6 MICROSCOPE SLIDES:

The microscope slides were prepared by following the method reported by Nidhi Natan *et al*²³. Slides based on silver and gold nanoparticles were prepared at different intervals of time. The absorbance spectra shown in Figure 42 and Figure 43 are for gold and silver nanoparticles at 12 hrs and show the absorbance spectra obtained for slides that were prepared without the acid washing step. Acid cleaning of the glass slides improves the reproducibility of the absorbance values and the magnitude of the absorbance values observed from the slides based on both gold and silver nanoparticles.

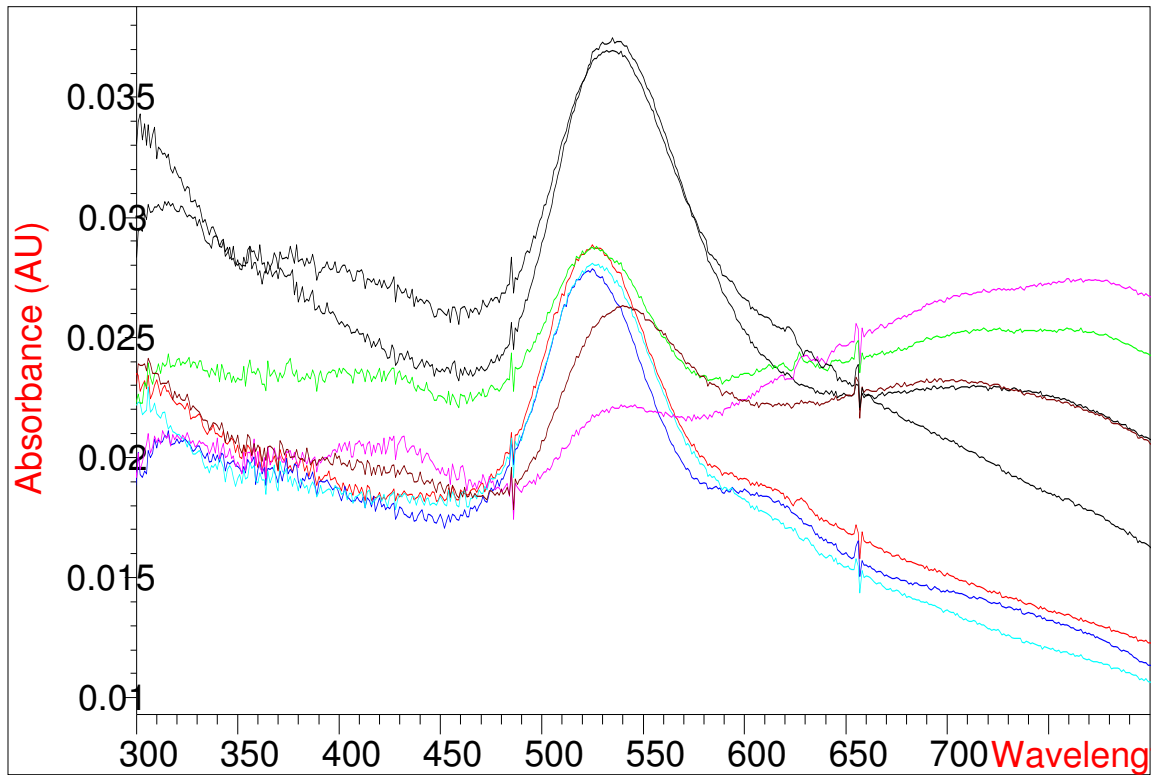


FIGURE 42 ABSORBANCE SPECTRA OF GOLD NANOPARTICLES ON GLASS SLIDES AT DIFFERENT WAVELENGTHS

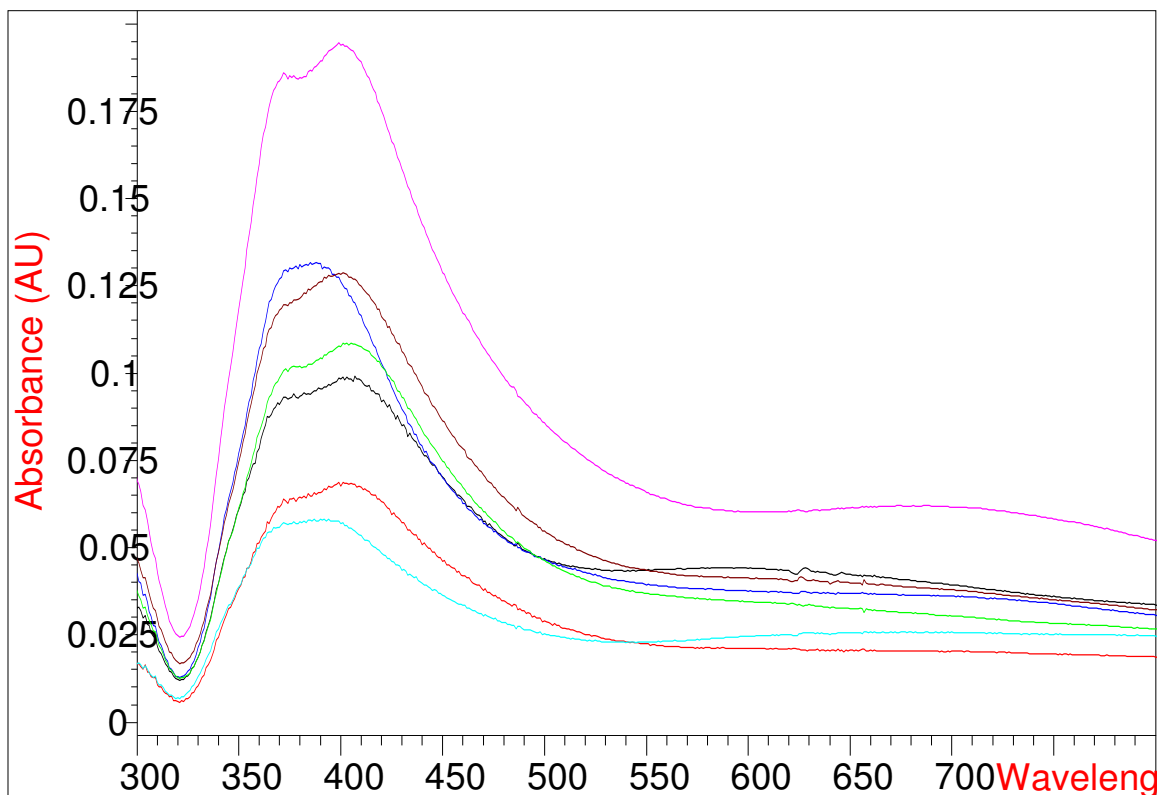


FIGURE 43 ABSORBANCE SPECTRA OF SILVER NANOPARTICLES ON GLASS SLIDES AT DIFFERENT WAVELENGTHS

From the absorbance spectra given in Figure 44 and 45 it is seen that the obtained spectra were clear and reproducible. The peaks obtained or the high absorbance values obtained for gold nanoparticles (Figure 44) at lower wavelengths (450 nm -550 nm) resulted due to the absorbance by the individual metal nanoparticles. After 550 nm it is observed that there is a decrease in the absorbance values and then at around 650 nm it is seen that the absorbance values tend to increase. This increase in the absorbance values is believed to be due to collective plasmon absorbance i.e. the absorbance at longer wavelengths is due

to clusters or aggregates of the nanoparticles. The increase in the absorbance values at higher wavelengths is often associated with SERS activity.

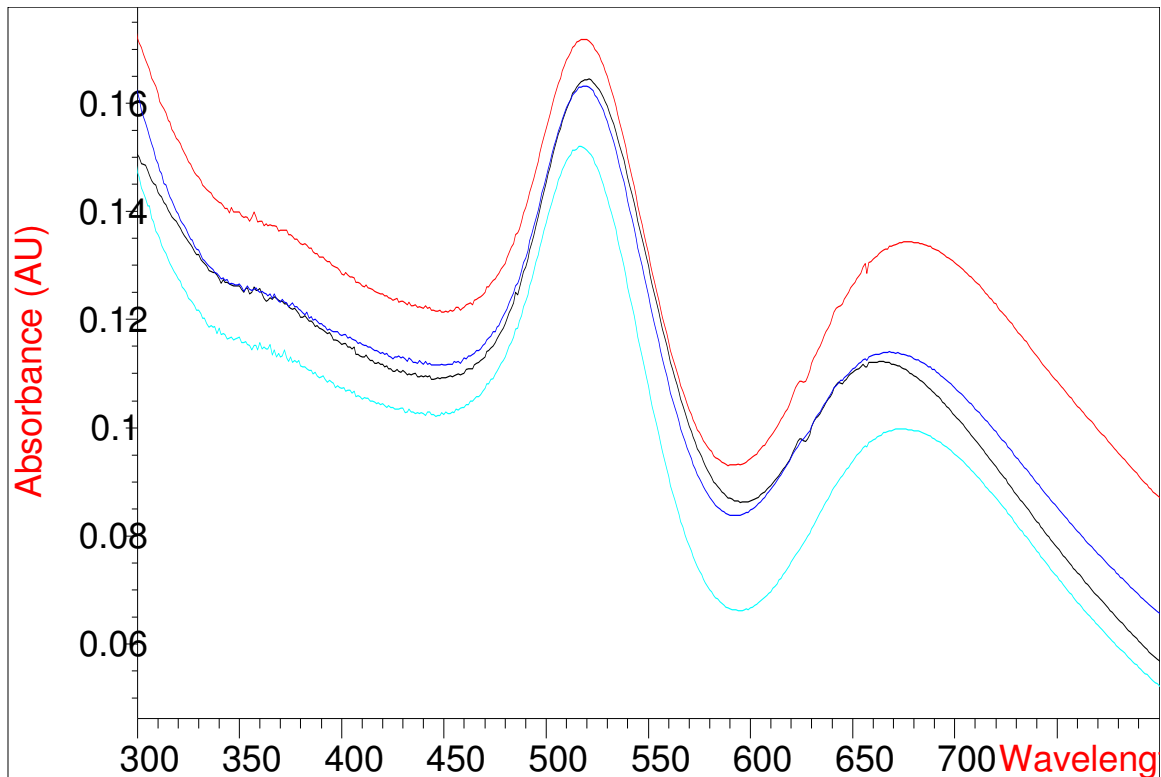


FIGURE 44 ABSORBANCE SPECTRA OF GOLD NANOPARTICLES ON GLASS SLIDES AFTER ACID WASH AT DIFFERENT WAVELENGTHS

From Figure 45, it is observed from the absorbance spectra that there is an increase in the absorbance values from 300 nm to 400 nm after which the values decreased. This stronger absorbance values at these wavelengths was due to the absorbance by individual silver metal nanoparticles. The absorbance values again start to increase at about 600 nm and this was due to apparent collective plasmon absorbance i.e. at longer wavelengths

there is an increase in the absorbance values because of the absorbance by aggregates of silver metal nanoparticles.

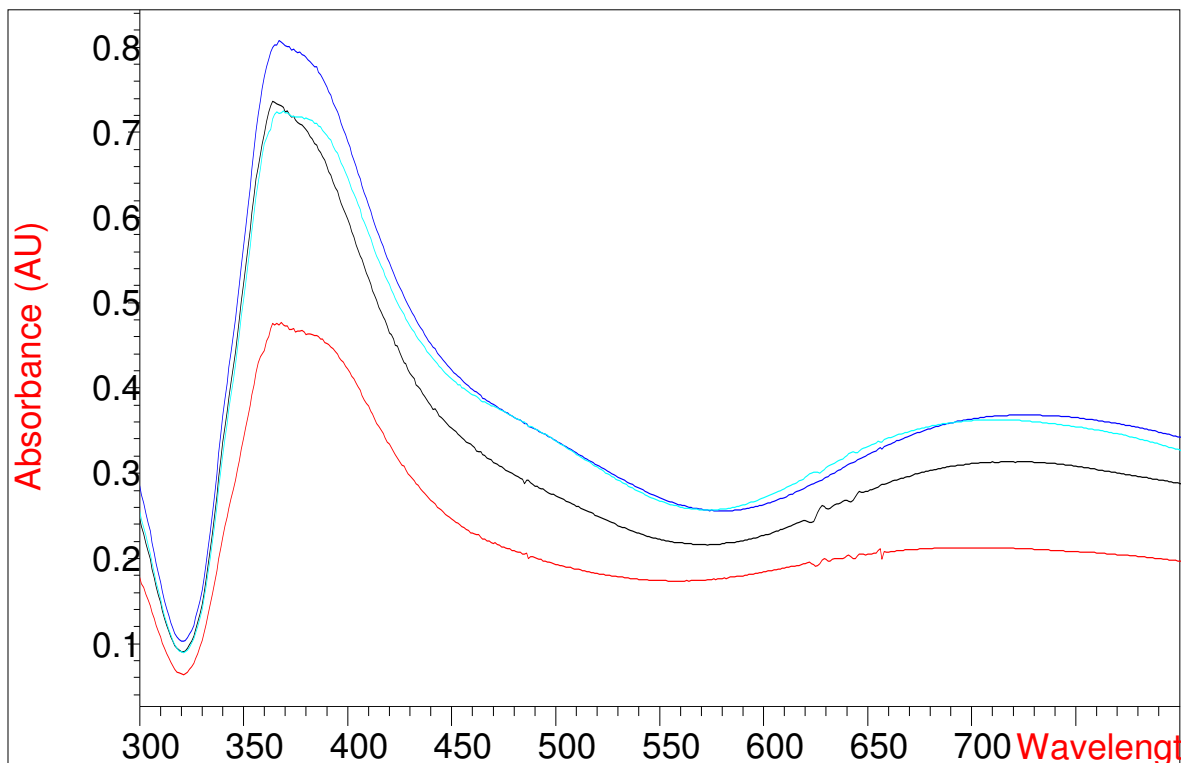


FIGURE 45 ABSORBANCE SPECTRA OF SILVER NANOPARTICLES ON GLASS SLIDES AT DIFFERENT WAVELENGTHS

Though good absorbance values were obtained from the silver and gold nanoparticles on glass slides, good SERs activity could not be observed.

3.7 POLY-L-LYSINE COATED SLIDES:

The substrates using poly-l-lysine slides were prepared by following a method described by Ratna Tantra *et al.*³⁶ The poly-l-lysine slides need no pretreatment such as drying or acid cleaning. The substrates are prepared simply by dipping the slides into the metal colloid solution and allowing the nanoparticles to bind to the lysine coated surface

of the slides. Absorbance spectra were collected for the slides at different times of exposure.

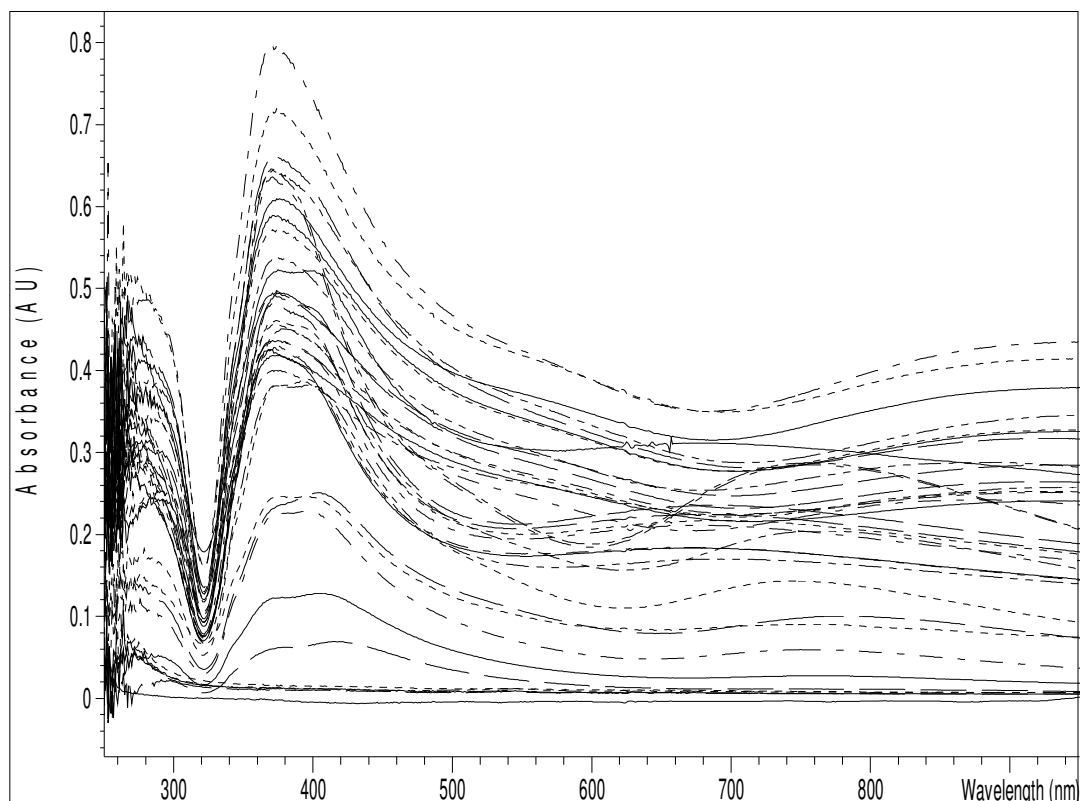


FIGURE 46 ABSORBANCE SPECTRA OF SILVER METAL NANOPARTICLES ON POLY-L-LYSINE SLIDES

SERS measurements were taken for R6G at different concentrations ranging from 1 mM to 1 μ M (Figure 47). The Raman spectra obtained did agree well with the peaks of R6G, but linearity was not observed. Therefore, more studies need to be done for achieving good linearity at lower concentrations of R6G on poly-l-lysine slides with silver metal nanoparticles.

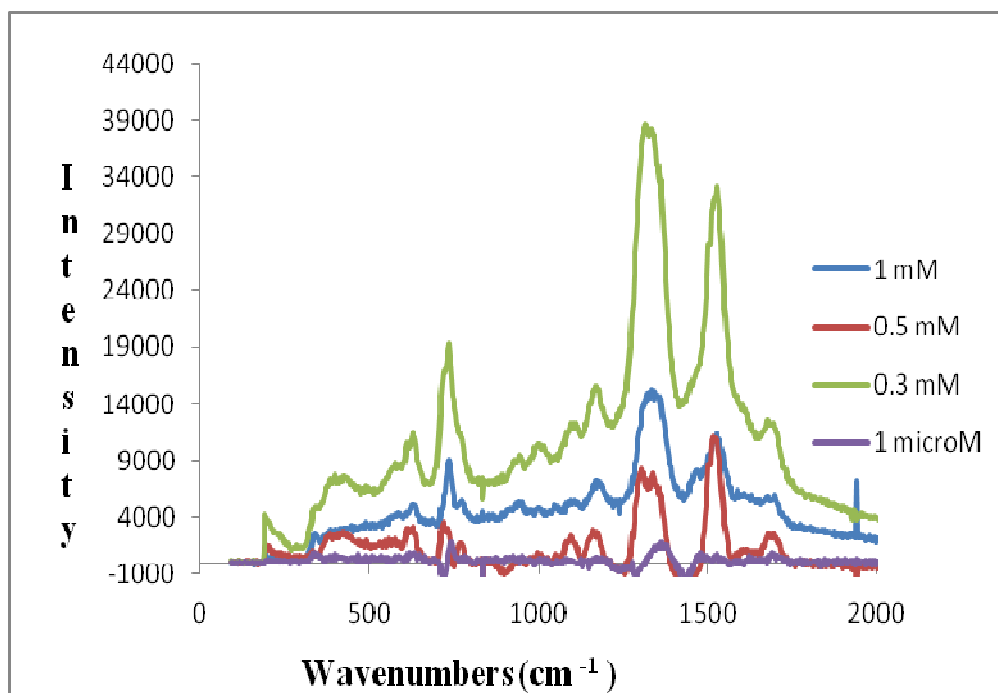


FIGURE 47 SERS MEASUREMENTS OF R6G ON POLY-L-LYSINE SLIDES WITH SILVER NANOPARTICLES AT DIFFERENT CONCENTRATIONS

4.0 CONCLUSIONS

Linearity of the SERS responses was observed for R6G compound between 1 μM – 0.1 μM concentrations on silver colloids. The maximum intensities were obtained at two wavenumbers 1346 cm^{-1} and 1519 cm^{-1} . From the calibration curve, a limit of detection of 0.03 μM was obtained with R6G in silver colloids. The trend of enhancement and absorbance data agreed well with the trend reported by *Souza et al.*²⁹ A maximum SERS enhancement was observed of 2×10^5 . However, no linearity was observed or obtained for R6G in gold metal nanoparticles.

Linearity of the SERS responses was observed for creatinine in silver colloids between the concentrations ranging from 1 mM to 20 mM. The limit of detection was found to be around 2 mM for creatinine in silver colloids. There was no clear trend in the absorbance data obtained and the enhancement was low. The results obtained did not agree with other reported LOD's. In the case of creatinine in gold metal nanoparticles, linearity could not be achieved even at high concentrations. There was no clear trend in the absorbance and the enhancement data obtained.

The spectral features obtained for imidazole in silver colloids agreed well with previous reported results. Linearity was observed at high concentrations ranging from 1 mM to 10 mM. No clear trend was observed in the absorbance data obtained. The sensitivity was low when compared to results reported previously. Linearity was not achieved for imidazole in gold metal nanoparticles even at high concentrations.

5.0 FUTURE STUDIES

SERS activity mainly depends on the metal nanoparticles (morphological characters) used i.e. their nanoparticle size, particle size distributions. SERS activity also depends on the concentration of the activator used. The colloids used in these studies comprise of many different sizes of nanoparticles. As a result, certain studies like evaluating the surface enhancement properties using absorption spectroscopy; microscopy should be performed to determine the optimum size of the metal nanoparticles at which the highest enhancement may be obtained.

Good linear dependence and absorbance data should be obtained at lower concentrations for creatinine and imidazole in both gold and silver nanoparticles.

The evaluation of SERS on solid substrates should be performed further. Optimization of substrates should be done for studying or detecting model compounds like Rhodamine6G species, benzoic acid species and other biological compounds. Different combinations of substrates should also be studied for SERS measurements of other compounds like pollutants, pharmaceutical products and biological compounds.

6.0 REFERENCES:

1. Roger M. Jarvis and Royston Goodacre. *Anal. Chem.* **2004**, 76, 40-47.
2. T.M. Cotton, Spectroscopy of Surface, in: R. J. H. Clark, R. E. Hester (Eds.), *Advances in Spectroscopy*, vol. 16, *John Wiley & Sons Ltd*, **1988**, p. 91.
3. Brandt, E. S.; Cotton, T. M. Investigations of Surfaces and Interfaces – Part B; Rossiter, B. W., Baetzold, R. C., Eds.; *John Wiley & Sons: New York*, **1993**; 633-718.
4. Moskovitis, M. *Rev. Mod. Phys.* **1985**, 57, 783-826.
5. Brike, R. L.; Lu, T.; Lombardi, J. R. In *Techniques for Characterization of Electrodes and Electrochemical Processes*; Varma, R., Selman, J. R., Eds.; *John Wiley & Sons: New York*, **1991**; 211-277.
6. Cotton, T. M.; Kim, J-H.; Chumanov, G. D. *J. Raman Spectroscopy.* **1991**, 22, 729-42.
7. Kneipp K, Kneipp H, Manoharan R, Itzkan I, Dasari RR, Feld MS. *Bioimaging* **1998**; 6; 104.
8. Kneipp K, Kneipp H, Manoharan R, Itzkan I, Dasari RR, Feld MS. *Single – Molecule Detection in Solution: Methods and Applications.* Wiley-VCH: Berlin, **2002**; 121.
9. Kneipp K, Kneipp H, Manoharan R, Itzkan I, Dasari RR, Feld MS. *J. Phys.: Condens. Matter* **2002**; 14: R597.
10. Brandt ES, Cotton TM. In *Surface-Enhanced Raman Scattering* (2nd edn), vol. IXB, Rossiter BW, Baetzold Rc (eds). *Wiley: New York*, 633-718.
11. Hill W, Wehling B, Klockow D. *Appl. Spectrosc.* **1999**; 53: 547.
12. Ayora MJ, Ballesteros L, Perez R, Ruperez A, Laserna J.J. *Anal. Chim. Acta* **1997**; 355: 15.
13. Lee HM, Kim MS, Kim K. *Vib. Spectrosc.* **1994**; 6: 205.
14. Kruszewski, S. *Surf. Interface Anal.* **1994**, 21, 830 – 838.
15. Xue G, Dong J. *Anal. Chem.* **1991**; 63:2393.
16. Hayat MA (ed). *Colloid gold: Principles, Methods and Applications*, Vols 1 and 2.
17. K. Faulds, W. e. Smith, D. Graham and R. J. Lacey. *Analyst.* **2002**, 127, 282-286.

-
18. Ramon A. Alvarez-Pueba, Elena Arceo, Paul J. G. Goulet, Julian J. Garrido, and Ricardo F. Aroca. *J. Phys. Chem. B* **2005**, 109, 3878-3792.
 19. Roark SE, Semin DJ, Lo A, Skodje RT, Rowlen KI. *Anal. Chim. Acta* **1995**, 307, 341.
 20. Roark SE, Rowlen KI. *Anal. Chem.* **1994**, 66, 261.
 21. Lefrant S, Baltog I, De La Chapelle ML, Baibarac M, Louarn G, Journet C, Bernier P. *Synth. Met.* **1999**, 100, 13.
 22. Jayaraj SE, Ramakrishnan V. *Specrosc. Lett.* **1999**, 32, 103.
 23. Zeisel D, Deckert V, Zenobi R, Vo-Dinh T. *Chem. Phys. Lett.* **1998**, 283, 381.
 24. Murphy T, Schmidt H, Kronfeldt HD. *Appl. Phys. B* **1999**, 69, 147.
 25. Keating CD, Kovaleski KM, Natan MJ. *J. Phys. Chem. B.* **1998**, 102, 9404.
 26. Constantino, C. J. L.; Lemma, T.; Antunes, P. A.; Aroca, R. *Anal. Chem.* **2001**, 73, 3674-3678.
 27. Garrell, R. L. *Anal. Chem.* **1989**, 61, 401A-411A.
 28. Creighton, J. A. In *Advances in Spectroscopy*; Clark R. J. H., Hester, R. E., Eds.; *John Wiley and Sons: Chicester*, **1988**; Vol. 16, 37-89.
 29. Glauco R. Souza, Carly S. Levin, Amin Hajitou, Renata Pasqualini, Wadih Arap and J. Houston Miller. *Anal. Chem.* **2006**, 78, 6232 – 6237.
 30. Andrea Lucotti, Giuseppe Zerbi. *Sensors and Actuators B* 121 **2007**, 356-364.
 31. D. Pritinski, S. L. Tan, M. Erol, H. Du, and S. Sukhishvili, *J. Raman Spectrosc.* **2006**, 37, 762.
 32. A. Kudelski, *Chem. Phys. Lett.* **2005**, 414, 271.
 33. Ying-Sing Li, Yu Wang, Jingcai Cheng. *Vibrational Spectrosc.* **2001**, 27, 65-74.
 34. Jung Sang Su and Jurae kim. *J. Raman. Spectrosc.* **1998**, 29, 143-148.
 35. P. G. Roth, R. S. Venkatachalam and F. J. Boerio. *J. Chem.. Phys.* **1986**, 85, 1150-1155.

-
36. Ratna Tantra, Richard j. C. Brown, Martin J. T. Milton, and Dipak Gohil., *J. Appl. Spec.*, **2008**, 62, 9, 992-999.
37. Xue, G.; Dai, Q.; Jiang, S. *J. Am. Chem. Soc.* **1988**, 110, 2393 – 2395.
38. Shi H, Ma Y, Ma Y., *Anal. Chim. Acta* **1995**, 312, 79-83.
39. W. Ranjith Premasiri, Richard H. Clarke, M. Edward Womble., *Lasers in Surgery and Medicine* **2001**, 28, 330 – 334.
40. Katherine C. Grabar, R. Griffith Freeman, Michael B. Hommer, and Michael J. Natan. *Anal Chem.*, **1995**, 67, 736 – 743.
41. Lee PC, Meisel D. *J. Phys. Chem.* **1982**, 86, 3391.
42. J. D. Guingab, B. Lauly, B. W. Smith, N. Omenetto, J. D. Winefordner. *Talanta* **2007**, 271-274.
43. Maria Oliver-Hoyo and Ralph W. Gerber. *Journal of Chemical Education.* **2007**, 84, 1174-1176.
44. Bosnick KA, Jiang J, Brus LE. *J. Phys. Chem. B.* **2002**, 106, 8096.
45. Nidhi Natan, Ashutosh Chilkoti. *Anal. Chem.* **2002**, 74, 504 – 509.